Guidelines for monitoring autophagy in *Caenorhabditis elegans*

Hong Zhang,[1,*] Jessica T Chang,[2] Bin Guo,[1] Malene Hansen,[2] Kailiang Jia,[3] Attila L Kovács,[4] Caroline Kumsta,[2] Louis R Lapierre,[2,†] Renaud Legouis,[5] Long Lin[1] Qun Lu,[1,‡] Alicia Meléndez,[6] Eyleen J O'Rourke,[7] Ken Sato,[8] Miyuki Sato,[9] Xiaochen Wang,[10] and Fan Wu[1]

[1]State Key Laboratory of Biomacromolecules; Institute of Biophysics; Chinese Academy of Sciences; Beijing, China; [2]Sanford-Burnham Medical Research Institute; Program of Development, Aging and Regeneration; La Jolla, CA USA; [3]Department of Biological Sciences; Florida Atlantic University; Jupiter, FL USA; [4]Department of Anatomy, Cell and Developmental Biology; Eötvös Loránd University; Budapest, Hungary; [5]Institute for Integrative Biology of the Cell; Paris-Saclay University; CEA; CNRS; Cedex, France; [6]Department of Biology; Queens College and the Graduate Center at the City University of New York; Flushing, NY USA; [7]Department of Biology; University of Virginia; Charlottesville, VA USA; [8]Laboratory of Molecular Traffic; Institute for Molecular and Cellular Regulation; Gunma University; Maebashi, Gunma, Japan; [9]Laboratory of Molecular Membrane Biology; Institute for Molecular and Cellular Regulation; Gunma University; Maebashi, Gunma, Japan; [10]National Institute of Biological Sciences; Beijing, China; [†]Current address: Brown University; Department of Molecular Biology; Cell Biology and Biochemistry; Providence, RI USA; [‡]Current address: Department of Pathology and Immunology; Washington University School of Medicine; St. Louis, MO USA

The cellular recycling process of autophagy has been extensively characterized with standard assays in yeast and mammalian cell lines. In multicellular organisms, numerous external and internal factors differentially affect autophagy activity in specific cell types throughout the stages of organismal ontogeny, adding complexity to the analysis of autophagy in these metazoans. Here we summarize currently available assays for monitoring the autophagic process in the nematode *C. elegans*. A combination of measuring levels of the lipidated Atg8 ortholog LGG-1, degradation of well-characterized autophagic substrates such as germline P granule components and the SQSTM1/p62 ortholog SQST-1, expression of autophagic genes and electron microscopy analysis of autophagic structures are presently the most informative, yet steady-state, approaches available to assess autophagy levels in *C. elegans*. We also review how altered autophagy activity affects a variety of biological processes in *C. elegans* such as L1 survival under starvation conditions, dauer formation, aging, and cell death, as well as neuronal cell specification. Taken together, *C. elegans* is emerging as a powerful model organism to monitor autophagy while evaluating important physiological roles for autophagy in key developmental events as well as during adulthood.

Introduction to Autophagy

Macroautophagy (hereafter referred to as autophagy) is an evolutionarily conserved catabolic process, involving the engulfment of a portion of the cytosol in a double-membrane structure, called the autophagosome, and its subsequent delivery to the lysosome for degradation.[1,2] Autophagy involves a series of dynamic membrane formation and fusion processes. Upon induction of autophagy, a crescent-shaped double-membrane sac, known as the phagophore, is initiated and formed; this sac further expands and eventually closes to generate a double-membrane compartment called the autophagosome. In higher eukaryotes, nascent autophagosomes undergo a maturation process by fusing with endocytic vesicles to form amphisomes that further fuse with lysosomes to yield autolysosomes, in which the inner membrane of the autophagosome, together with the sequestrated materials, is degraded and recycled. In response to various stress conditions, autophagy nonselectively degrades bulk cytosol for cell survival. Autophagy can also selectively remove damaged or superfluous organelles, protein aggregates or invading pathogens, functioning as a quality control system.[3]

Genetic screens in *Saccharomyces cerevisiae* initially identified a set of *ATG* (autophagy-related) genes that are essential for the formation of autophagosomes, laying the groundwork for our understanding of the molecular mechanism of autophagy.[1,2] Atg proteins form distinct complexes that act at different steps of autophagosome biogenesis.[1,2] The induction and nucleation of phagophores depends on the Atg1 serine/threonine protein kinase complex, including Atg1, Atg13, and the Atg17-Atg31-Atg29 subcomplex, and the class III phosphatidylinositol 3-kinase Vps34 complex. Expansion of phagophores into autophagosomes requires 2 ubiquitin-like conjugation systems. First, the ubiquitin-like protein Atg8 is conjugated to phosphatidylethanolamine (PE) through the sequential actions of the E1-like

enzyme Atg7 and the E2-like conjugating enzyme Atg3, while the second ubiquitin-like protein Atg12 is conjugated to Atg5 via the actions of Atg7 and the E2-like enzyme Atg10. The Atg12-Atg5 conjugates further associate with Atg16 to form a multimeric complex, which regulates Atg8–PE conjugation and its localization. Following completion of autophagosomes, Atg8 on the outer membrane is cleaved off by the cysteine protease Atg4 and recycled, while Atg8 on the inner membrane is transported into the vacuole for degradation.[1,2] In multicellular organisms, the autophagic machinery is more evolved and requires not only orthologs (or multiple orthologs) of yeast *ATG* genes but also genes whose homologs are absent in yeast but conserved in mammals.[4-6] Genetic screens in *C. elegans* have identified several metazoan-specific autophagy genes. For example, *epg-3/VMP1* (mammalian homolog), *epg-4/EI24* and *epg-6/WIPI4* are involved in progression of omegasomes/phagophores into autophagosomes, while *epg-5/EPG5* is essential for the formation of degradative autolysosomes.[4,5] Although many autophagy genes have been identified, how these genes act coordinately to mediate the formation and maturation of autophagosomes remains largely unknown.

C. *elegans* as a Model to Study Autophagy

Caenorhabditis elegans is a self-fertilizing hermaphrodite nematode species. Males, which arise spontaneously at low frequency (0.1%), can also fertilize hermaphrodites to produce cross progeny. The life cycle of *C. elegans* is comprised of the embryonic stage, 4 larval stages (L1-L4), and the reproductively mature adult stage, during which the animal will age and die within 2–3 wk in favorable conditions. When early larvae are exposed to harsh environmental conditions, they enter the dauer diapause, which enables them to survive 4 to 8 times the normal 3-wk life span. *C. elegans* has many advantages for genetic analysis: it is transparent, small, easy to culture, amenable to genetic crosses, has a short reproductive cycle (∼3 d) with hundreds of progeny per adult, an invariant cell lineage (959 somatic cells in hermaphrodites), a stereotypical developmental program, highly differentiated somatic tissues, and diverse behavioral and physiological phenotypes. Powerful genetic tools and mature methodologies such as forward genetic screens, generation of transgenic animals and RNA interference (RNAi) in a tissue-specific fashion have been developed that have greatly facilitated research in *C. elegans.* These advantages make *C. elegans* an ideal genetic model to study a variety of biological processes, which can be extrapolated to research in more complex organisms. Indeed, studies of *C. elegans* developmental and physiological processes led to the discovery of the apoptotic cell death machinery, siRNA-mediated mRNA degradation, and miRNA-mediated gene silencing. Additionally, *C. elegans* has been instrumental in elucidating many well-conserved signaling pathways, such as those involving RAS, WNT, INS (insulin)/IGF1, and TGFB.

Autophagy in *C. elegans* occurs in many cell types and plays an essential role in many developmental and physiological processes, including survival of animals under nutrient restricted conditions, removal of a variety of protein substrates, degeneration of 6 touch receptor neurons caused by toxic ion-channel variants, dauer formation, the aging process, and prevention of bacterial infection.[4,7-14] These processes will be discussed in detail below. Autophagic removal of a variety of protein substrates during embryogenesis has established *C. elegans* as a model suitable for genetic screens for essential autophagy genes.[4-6] In addition to highly conserved yeast Atg proteins, such genetic screens in *C. elegans* have identified metazoan-specific components of the basal autophagy pathway (**Table 1**), greatly expanding our molecular understanding of autophagy in higher eukaryotes.[6] Genes that are distantly related homologs of yeast *ATG* genes or that have no yeast counterparts include *epg-1*, *-3*, *-4, -5, -6, -8,* and *epg-9*.[4,5,15-17] *C. elegans* also contains 2 homologs of yeast *ATG4*, *ATG16,* and *ATG8*, which confers another layer of complexity on the autophagic machinery. A detailed summary of the role of these genes in the autophagy pathway can be found in recent reviews.[6,18] Epistasis genetic analysis places these autophagy genes in a hierarchical order in the pathway for degradation of protein aggregates, a process known as aggrephagy (**Fig. 1**).[5,6] The sequential involvement of these genes in the aggrephagy pathway in *C. elegans* resembles the hierarchical order of Atg/ATG proteins that are recruited to the autophagosome formation site in yeast and mammalian cells.[19,20]

Classical Assays to Monitor Autophagy

Assays for monitoring autophagy activity have been extensively described in yeast and mammalian cell lines.[21,22] Atg8/LC3 (a mammalian Atg8 homolog) is widely used as a marker to monitor autophagy activity.[21,22] The PE-conjugated form of Atg8/LC3 is localized to both the inner and outer membranes of the phagophore. Thus, Atg8/LC3 associates with autophagosomal membranes upon autophagy induction. Degradation of autophagy substrates such as SQSTM1/p62 (sequestosome 1) and ubiquitinated proteins in mammalian cells can also be used to monitor autophagy.[21,22] Moreover, detailed morphological characterization of autophagic structures can be achieved by the high magnification and resolution images of transmission electron microscopy (TEM).[21,22] The complex and multistep autophagy process, however, cannot be analyzed by any single assay, especially those considered steady-state in nature and thus not reporting on autophagic flux per se. Instead, a combination of assays is required for measuring autophagy activity.

Despite *C. elegans* emerging as an important model to study autophagy at the molecular level and to reveal functions of autophagy during development and in physiology, it is not easily amenable to the main methods of traditional autophagy studies such as cell fractionation and TEM.[23] In addition, studying autophagy in a multicellular organism is complicated by the heterogeneity of cell types, spatial and temporal cell fates, and differential response to stress conditions in different tissues. In order to study autophagy in *C. elegans*, researchers rely heavily, and in most cases solely, on the expression pattern of reporters for the Atg8/LC3 ortholog LGG-1. This assay has many limitations (see

Table 1. Autophagy genes in yeast, mammals and *C. elegans*.

Yeast *ATG* gene	Mammalian *ATG* homolog(s)	*C. elegans* ATG homolog(s)		
		gene	mutant allele(s)[a,b]	Ref[e]
ATG1	ULK1	unc-51	e369	85
ATG2	ATG2A, ATG2B	atg-2	bp576	5
ATG3	ATG3	atg-3	bp412	7
ATG4	ATG4A, ATG4B, ATG4C, ATG4D	atg-4.1	bp501	26
		atg-4.2	tm3948[c]	26
ATG5	ATG5	atg-5	bp484	27
ATG7	ATG7	atg-7	bp422, bp290	7
ATG8	LC3, GABARAP, GABARAPL1, GABARAPL2	lgg-1	bp500, tm3489	4, 25
		lgg-2	tm5755	25
ATG9	ATG9	atg-9	bp564	5
ATG10	ATG10	atg-10	bp421	7
ATG12	ATG12	lgg-3	tm1642	
ATG13	ATG13	epg-1	bp417	15
ATG14	ATG14	epg-8	bp251, ok2561	16
ATG16	ATG16L1, ATG16L2	atg-16.1	gk668615[d]	27
		atg-16.2	bp636, ok3224	27
ATG17	RB1CC1			
ATG18	WIPI1, WIPI2, WIPI3, WIPI4	atg-18	bp594, gk378	4, 31
		epg-6	bp242	5
VPS30/ATG6	BECN1	bec-1	bp613, ok700	31, 86
VPS34	PIK3C3	vps-34	h741	87
	VMP1	epg-3	bp405	4
	EI24	epg-4	bp425	4
	EPG5	epg-5	bp450, tm3425	4
	ATG101	epg-9	bp320	17
		epg-2	bp287	4
		epg-7	bp586, tm2508	35

[a]The null mutants for *bec-1*, *epg-8*, *vps-34*, *atg-7*, *lgg-1* and *lgg-3* are lethal.
[b]*bec-1(bp613)* and *atg-18(bp594)* are hypomorphic mutants and exhibit a weaker defect in degradation of PGL granules and SQST-1 aggregates than their corresponding null mutants.
[c]*atg-4.2(tm3948)* mutants show no defect in degradation of PGL granules and SQST-1 aggregates.
[d]*atg-16.1(gk668615)* mutants show a very weak defect in degradation of PGL granules and SQST-1 aggregates.
[e]The molecular lesions in each listed mutant and more mutant alleles for each gene can be found in the references.

below) and cannot by itself serve as a marker to determine whether autophagy activity is elevated or impaired. Here we summarize currently available assays to monitor autophagy during *C. elegans* development and physiology, while pointing out their limitations.

Monitoring Autophagy During *C. elegans* Embryogenesis

After passing from the oviduct into the spermatheca, mature oocytes become fertilized by fusion with sperm. Fertilized embryos in the uterus undergo several rounds of cell division (reaching approximately the 30-cell stage) before they are laid through the vulva. The *C. elegans* embryo is enclosed in a hard eggshell and remains the same size from the one-cell stage to the 558-cell stage, resulting in a gradual reduction of cell size. Cell-fate specification and morphogenesis occur in a spatially- and temporally-specific pattern. According to their appearance, embryos can be classified into pre-comma, comma, 2-fold, 3-fold, and 4-fold stages. The surrounding eggshell is impermeable to most solutes. Consequently, the development of *C. elegans* embryos is independent of external nutrients and mainly relies on degradation of maternally-loaded yolk. Therefore, autophagy occurs under
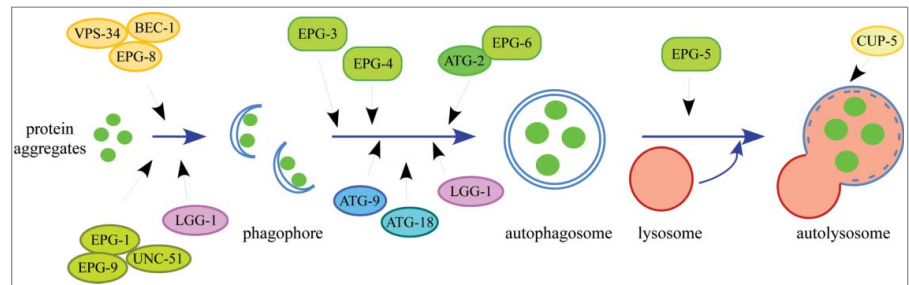

Figure 1. The hierarchical order of autophagy genes in the aggrephagy pathway.

physiological conditions without being affected by external nutrient availability in *C. elegans* embryos.

LGG-1 puncta and levels of LGG-1

C. elegans contains 2 Atg8 homologs, encoded by *lgg-1* and *lgg-2*, both of which are involved in autophagy.[4,10,24,25] In wild-type *C. elegans*, LGG-1 is synthesized as a precursor that is processed by the cysteine proteases ATG-4.1 and ATG-4.2 at a conserved glycine residue at amino acid 116, to release the final 7 C-terminal residues and generate LGG-1-I, which is further conjugated to PE via the sequential actions of ATG-7 and ATG-3 to give rise to LGG-1-II.[26] Levels of LGG-1 and also formation of LGG-1 puncta can be examined to monitor autophagy during embryogenesis.

Levels of LGG-1-I and -II

Based on molecular weight and lipid modification status, 3 forms of LGG-1, i.e., LGG-1 precursor, LGG-1-I and LGG-1-II, can be separated by SDS-PAGE (**Fig. 2A**). LGG-1 precursors are absent in wild-type embryos, but accumulate in *atg-4.1* mutants (**Fig. 2A**).[26] Both LGG-1-I and LGG-1-II are present in wild-type embryos, whereas LGG-1-II is undetectable in *atg-3* and *atg-5* mutants (**Fig. 2A**).[4,27] When autophagy is blocked at the step of autophagosome formation such as in *epg-3, -4,* and *-6* mutants, or at the maturation step such as in *epg-5* mutants, levels of both LGG-1-I and LGG-1-II are elevated compared to wild-type animals (**Fig. 2A**).[4,5] LGG-1-II also accumulates in response to mutation of autophagy genes involved in autophagosome formation, including in UNC-51/Atg1 kinase complex mutants, VPS-34 PtdIns3P lipid kinase complex mutants, and in *atg-18* and *atg-9* mutants.[4,16,17] Therefore, an increase in levels of lipidated LGG-1 can result from a block of autophagy.

Cautionary notes: In immunoblotting assays, LGG-1-II migrates faster than LGG-1-I and can be separated by 13% SDS-PAGE without special treatments or other gel conditions such as the inclusion of urea. LGG-1-I is stable and appears not to be affected by sample preparation through repeated freeze-thaw cycles. Levels of LGG-1-II vary at different developmental stages.
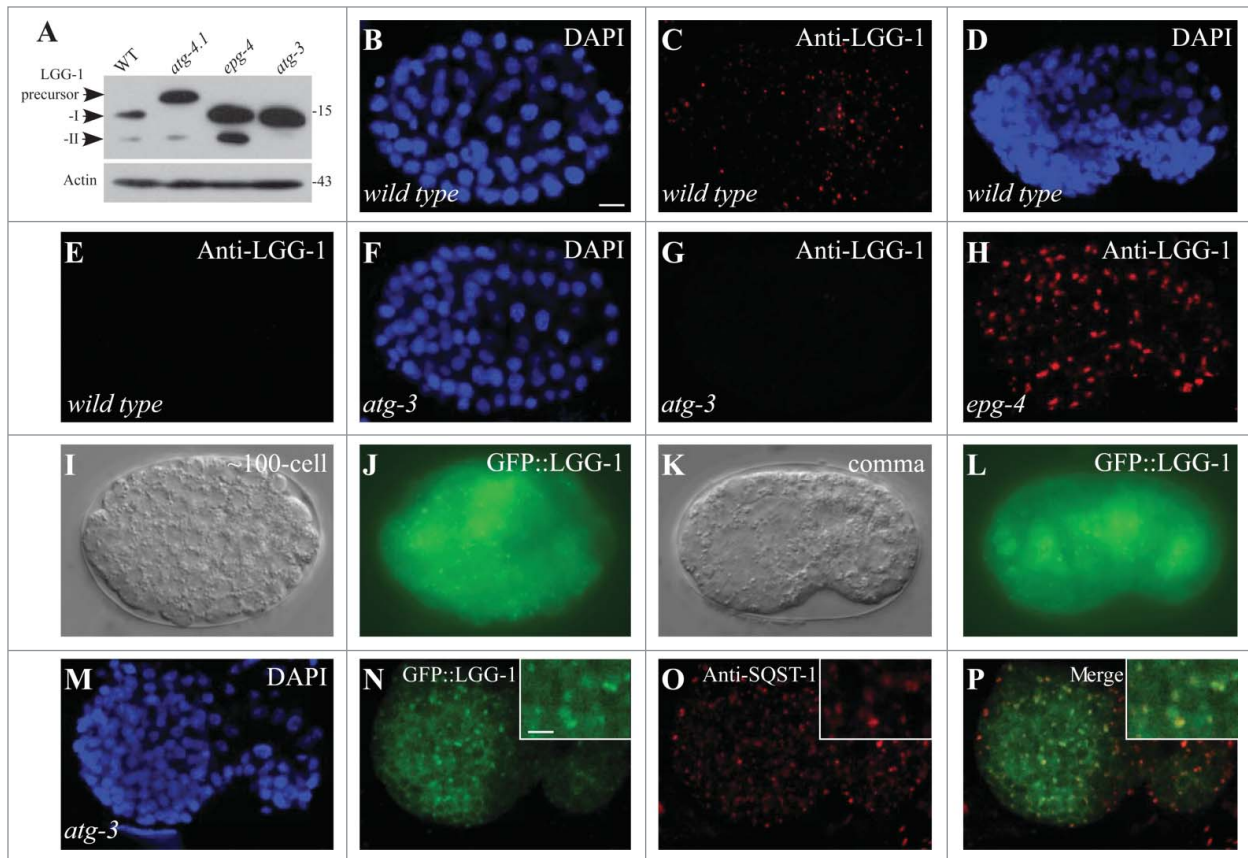

Figure 2. LGG-1 pattern during embryogenesis. (**A**) LGG-1 precursor, LGG-1-I (unlipidated form) and LGG-1-II (lipidated form) in wild-type and *atg-4.1*, *epg-4* and *atg-3* mutant embryos. (**B–E**) LGG-1 forms punctate structures at the ~100-cell stage ((**B**)and C), but these structures disappear at the comma stage in wild-type embryos ((**D**)and E). ((**B**)and D) DAPI images of the embryos shown in ((**C**)and E), respectively. ((**F**)and G) LGG-1 puncta are absent in *atg-3* embryos. (**F**) DAPI image of the embryo shown in (**G**). (**H**) LGG-1 accumulates into enlarged cluster-like structures in *epg-4* embryos. (**I–L**) GFP::LGG-1 is largely diffuse in the cytoplasm with some punctate structures. ((**I**)and K) DIC images of the embryos shown in ((**J**)and L), respectively. (**M–P**) GFP::LGG-1 forms aggregates in *atg-3* mutant embryos, which colocalize with SQST-1 aggregates. Inserts show magnified views. (**M**) DAPI image of the embryo shown in (**N–P**). Scale bar: 5 μm (**B-P**); 2.5 μm (inserts in **N–P**). *C. elegans* embryos remain the same size during embryogenesis. Thus, the scale bar is only shown once in each figure.

For immunoblotting assays, embryos need to be synchronized, which can be roughly achieved by growing the embryos after bleaching gravid hermaphrodites. Wild-type embryos at the same stage should serve as a control to compare LGG-1-II levels. Detection of LGG-1 levels by immunoblotting assays can be complicated by the heterogeneity of cell types in embryos. For example, the large accumulation of LGG-1-II in a few cells cannot be differentiated from a smaller increase of LGG-1-II in a larger number of other cells. Also, as noted above, impaired autophagy could lead to accumulation of LGG-1-II; thus, other assays are required for measuring autophagy.

Anti-LGG-1 staining and GFP::LGG-1 puncta

Immunostaining with anti-LGG-1 antibody or expression of the GFP::LGG-1 reporter can be examined to monitor distribution of total LGG-1 in *C. elegans* embryos.[4,10,28] During embryogenesis, LGG-1 puncta, detected by anti-LGG-1, display a dynamic pattern. LGG-1 puncta are mostly formed between the ~100 and 200-cell stages (**Fig. 2B-E**). The number of puncta dramatically decreases as development proceeds with a minimum detected at the 4-fold stage.[4,5]

In addition to the 100- to 200-cell stages, LGG-1-positive structures are formed intensively around penetrating sperm components in early one-cell-stage embryos.[29,30] These LGG-1-positive structures appear approximately 20 min after fertilization (during meiosis II) and first cluster around the paternal DNA. They start to disperse in the cytoplasm during pronuclear break down, are randomly distributed to blastomeres, and gradually disappear by the 8-cell stage. These LGG-1-labeled structures, which are larger than those formed in the later embryonic stages, specifically engulf paternal mitochondria and membranous organelles (MOs), which are sperm-specific post-Golgi organelles.[29,30]

LGG-1 exhibits distinct patterns in different autophagy mutants. In mutants of *atg-3* and *atg-7*, which are required for LGG-1 conjugation to PE, no LGG-1 puncta are detected (**Fig. 2F and G**), indicating that LGG-1-II accumulates on autophagic structures and contributes to the formation of LGG-1 puncta.[4] Consistent with this, mutant LGG-1(G116A), in which the glycine at position 116 is mutated to alanine, preventing PE-conjugation, is diffusely localized in the cytoplasm and does not form puncta.[25] LGG-1 puncta are also absent in *atg-5* and *atg-10* mutants.[4,27] In mutants of the Atg1 complex, including *unc-51/ULK1, epg-1/ATG13,* and *epg-9/ATG101*, LGG-1 puncta are absent in most cells, but LGG-1 accumulates into large aggregates in several cells.[17] The identity of these LGG-1-positive structures has yet to be characterized. In mutants of the PtdIns3K complex, including *epg-8/ATG14* and *bec-1/BECN1*, LGG-1 forms puncta, but the intensity is weaker.[6] In *epg-3, epg-4, epg-6,* and *atg-2* mutants, which have defects in the progression of omegasomes to autophagosomes, LGG-1 puncta dramatically accumulate and form cluster-like structures that are largely colocalized with protein aggregates (**Fig. 2H**).[4,5] LGG-1 puncta also accumulate in other autophagy mutants, including *atg-18* and *epg-5*.[4,5] In these autophagy mutants, LGG-1 puncta persist into late stages of embryogenesis. *ogt-1* mutant embryos, which show elevated autophagy activity, also exhibit increased numbers of LGG-1 puncta.[31] Therefore, an increase in the number of LGG-1 puncta during embryogenesis could be due to either impaired or elevated autophagy activity.

GFP::LGG-1, driven by its own promoter, also exhibits a dynamic pattern resembling endogenous LGG-1 puncta during embryogenesis in wild-type animals (**Fig. 2I–L**). GFP::LGG-1 is largely diffuse in the cytoplasm but forms some punctate structures, which are still present in comma stage embryos (**Fig. 2K and L**).[7] GFP::LGG-1 accumulates in the autolysosomes in *cup-5* mutants, which show impaired lysosomal function.[32] The autophagosomes enclosing sperm components in early stage embryos can also be labeled by GFP::LGG-1, and thus, strong accumulation of the GFP signal is visible in the posterior pole of the 1-cell-stage embryo.[29] In addition, several small GFP::LGG-1-positive puncta are observed in the cytoplasm of oocytes and early embryos, which may represent basal autophagic activity. In *atg-3* and *atg-7* mutants, in which LGG-1 puncta detected by anti-LGG-1 are absent, GFP::LGG-1 still forms aggregates that colocalize with protein aggregates that can be labeled by the *C. elegans* SQSTM1-related protein SQST-1 (**Fig. 2M–P**).[15] This indicates that GFP::LGG-1, like GFP::LC3 in mammalian cells, can also be incorporated into protein aggregates. Therefore, under certain circumstances, GFP::LGG-1 may not serve as a reliable marker to determine autophagy activity during embryogenesis.

Cautionary notes: The number of LGG-1 puncta varies dramatically during embryogenesis and thus embryos at the same developmental stage should be compared. An increased number of LGG-1 puncta and levels of PE-LGG-1 can result from either a block in or induction of autophagic activity and can be detected in mutants with a defect in early steps of autophagosome formation (i.e., accumulation of enlarged phagophore membranes in *epg-3* and *epg-4* mutants) or in a late step of the autophagy pathway such as defective autolysosome function. Furthermore, lipidated LGG-1 also accumulates on unknown structures such as in mutants of the Atg1 complex.[17] Therefore, LGG-1 puncta formation should not be used as the sole marker for assaying autophagy, as is the case in mammalian cells.[21,22] Furthermore, GFP::LGG-1 transgenes, which may cause overexpression of *lgg-1*, might interfere with autophagy (as shown in other species). When possible, antibody staining should be preferred and the overexpression level should be minimized using endogenous promoters and single-copy transgenes.

Analyses of autophagosomes using LGG-2

LGG-2 has been much less characterized than LGG-1, but it can be used as a convenient alternative marker to monitor autophagy activity during development.[24,25] Unlike *lgg-1*, *lgg-2* is not essential for development and fertility (**Table 1**).

Immunostaining with anti-LGG-2 antibodies or expression of a GFP::LGG-2 reporter can be examined to monitor distribution of LGG-2 in *C. elegans* embryos or larvae (**Fig. 3A**).[24,25] The number of LGG-2 puncta is altered in mutants that affect autophagy (e.g., *atg-7* or *epg -3, -4, -5*) (**Fig. 3A and B**). Electron microscopy has shown that LGG-2 is localized on autophagic membranes and
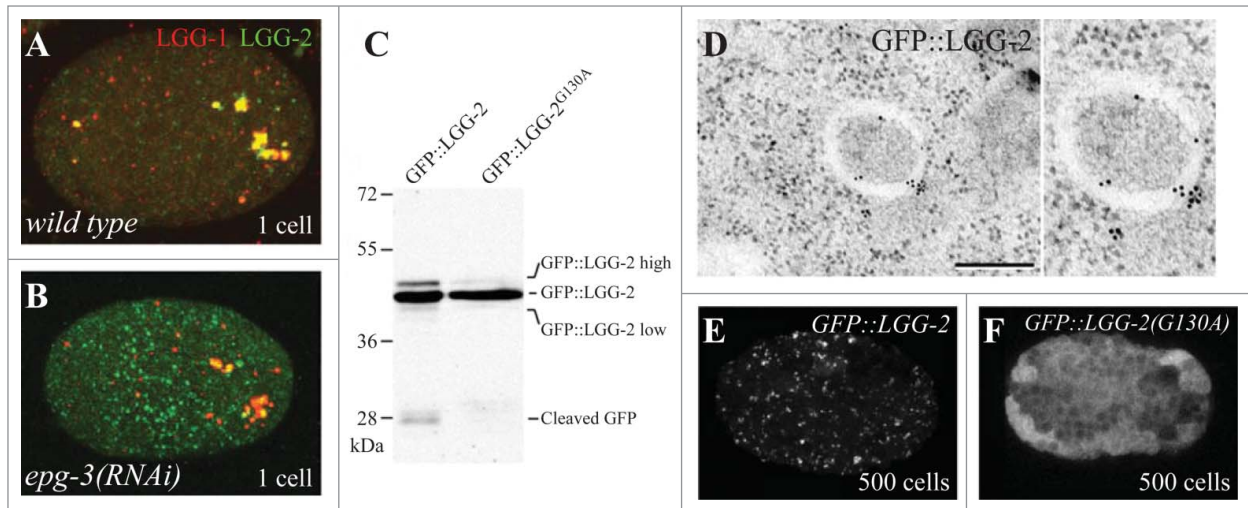
Figure 3. LGG-2 puncta during embryogenesis. ((**A**)and **B**) Confocal images of LGG-1 (red) and LGG-2 (green) in wild-type and *epg-3* 1-cell embryos. (**C**) Western blot of protein extracts from mixed-stage GFP::LGG-2 and GFP::LGG-2^{G130A} transgenic worms incubated with anti-GFP antibody. (**D**) Electron micrographs of GFP::LGG-2 embryos incubated with anti-GFP antibodies. The right panel shows a magnified view of the autophagosome. Scale bar: 200 nm. ((**E**)and **F**) Confocal images of GFP::LGG-2 and GFP::LGG-2^{G130A} in 500-cell embryos. GFP::LGG-2 localizes in both a punctate and a diffuse pattern while GFP::LGG-2^{G130A} is diffusely localized in the cytosol. This figure was previously published in references 24 and 25 and is reproduced by permission of Elsevier and Landes Bioscience.

can be detected early during the elongation of phagophores (**Fig. 3D**).[25] Immunofluorescence analysis revealed the presence of 3 types of punctate structures in the embryo, LGG-1-positive puncta, LGG-2-positive puncta, and double-positive puncta,[25] indicating that they could define different types of autophagic structures or that LGG-1 and LGG-2 are sequentially recruited to autophagic structures. Western blot analysis of animals expressing GFP::LGG-2 shows a major GFP-positive band corresponding to the fusion proteins and 2 additional minor bands, which could correspond to post-translational modifications, but the lipidated form has not been formally identified (**Fig. 3C**).[24] The nonconjugatable GFP::LGG-2^{G130A} exhibits a diffuse localization pattern in the cytoplasm (**Fig. 3E and F**).

Cautionary notes: Analyses of LGG-2 levels by immunoblotting and GFP::LGG-2 should be interpreted with the same precautions as those for LGG-1. The number of LGG-2 puncta varies during development and thus animals at the same developmental stage should be compared. Antibodies against LGG-2 have only been used to characterize autophagy in the early embryo, and their specificity at other developmental stages remains to be determined. Because the process of lipidation of LGG-2 has not been further investigated, western blot analyses of GFP::LGG-2 alone are not sufficient to make conclusions about autophagic flux.

Monitoring autophagy substrates

During *C. elegans* embryogenesis, a variety of protein substrates, including PGL granules (containing the germline P granule components PGL-1 and PGL-3 and the receptor protein SEPA-1) and SQST-1, are degraded by autophagy.[4,7] Thus, levels of these autophagy substrates can be determined to monitor autophagy. The morphology and distribution pattern of these protein substrates are distinct in different autophagy mutants,

and this has been used to establish the hierarchical order of autophagy genes in the aggrephagy pathway.[5,6]

P-granule proteins PGL-1 and PGL-3

During *C. elegans* embryogenesis, maternally-loaded P granules are exclusively localized in germline precursor cells (**Fig. 4A and B**).[33] During early asymmetric divisions that give rise to the germline precursor cells P1, P2, P3, and P4, P granules are also partitioned into somatic blastomeres but are quickly removed.[7,33] The P granule components PGL-1 and PGL-3 are selectively removed from somatic cells by autophagy.[7] In autophagy mutants, PGL-1 and PGL-3 accumulate into aggregates in somatic cells (**Fig. 4C and D**).[7] Formation of PGL-1 and PGL-3 granules in somatic cells can be detected by immunostaining using anti-PGL-1 and PGL-3 antibodies or by following the corresponding *gfp* reporters. Levels of PGL-1 and PGL-3 can also be determined by immunoblotting assays using embryonic extracts.

Cautionary notes: Endogenous PGL granules, detected by anti-PGL-1 and PGL-3 antibodies, are absent in somatic cells in wild-type embryos. However, the widely used *gfp::pgl-1* reporter, which is driven by the germline-specific *pie-1* promoter, is nonspecifically expressed in hypodermal cells at late embryonic stages, resulting in the formation of some small GFP::PGL-1 aggregates. Thus, early embryos, i.e., comma stage or earlier, should be used for detecting somatic GFP::PGL-1 granules, before *gfp::pgl-1* is expressed ectopically. The experiments should be performed at 20 °C, since PGL-1 and PGL-3 form aggregates in somatic cells if the embryos are raised at higher temperatures.

In addition to autophagy mutants, somatic-to-germline cell fate transformation mutants also show formation of P granules in somatic cells. For example, somatic cells adopt germline cell traits in *lin-35* and other synthetic multivulva (synMuv) B mutants or

in animals with impaired proteasome activity.[7,34] In cell fate transformation mutants, P granules are present in a subset of cells (e.g., hypodermal cells and intestinal cells) at the larval stage and usually have a perinuclear localization, while P granules are dispersed in the cytoplasm in most, if not all, somatic cells in autophagy mutant embryos.

During *C. elegans* embryogenesis, germ blastomeres, especially P1 (at the 2-cell stage) and P2 (at the 4-cell stage), contain a huge amount of P granules. P4 divides once to generate 2 germ precursor cells, Z2 and Z3, which remain quiescent during embryogenesis. P granules persist in Z2 and Z3 throughout embryogenesis. To determine levels of PGL-1 and PGL-3 in immunoblotting assays, embryos after the generation of the Z2 and Z3 cells (at the ~100 cell stage) should be used to minimize the relative contribution of PGL-1 and PGL-3 from germline cells. Z2 and Z3 proliferate from the late L1 stage onward to generate germ cells, in which P granules are synthesized. These germ cells, which increase in number as development proceeds, are stored in the gonad. Thus, larval animals should be separated from embryos in immunoblotting assays.

The receptor protein SEPA-1

The self-oligomerizing protein SEPA-1 acts as the receptor for the formation of PGL-1 and PGL-3 granules and also for their autophagic degradation.[7] SEPA-1 directly associates with PGL-3 and LGG-1.[7] SEPA-1 is also selectively removed by autophagy, which is independent of PGL-1 and PGL-3.[7] In wild-type embryos, the number of SEPA-1 aggregates is dramatically decreased as development proceeds. A large number of SEPA-1 aggregates are detected at the ~100-cell stage and only a few SEPA-1 aggregates remain at the 200-cell stage (**Fig. 4E and F**). SEPA-1 aggregates disappear from the comma stage onward (**Fig. 4G and H**).[7] Inhibition of autophagy causes accumulation of SEPA-1 into a large number of aggregates that persist throughout embryogenesis (**Fig. 4I and J**).[7] In autophagy mutants, SEPA-1 completely colocalizes with PGL-1 and PGL-3 in somatic cells, forming aggregates termed PGL granules.[7] SEPA-1::GFP exhibits the same dynamic distribution pattern as endogenous SEPA-1 detected with an anti-SEPA-1 antibody.[7] Levels of SEPA-1 or SEPA-1::GFP in embryonic extracts can also be determined in immunoblotting assays. Elevated autophagy activity during embryogenesis may facilitate the removal of SEPA-1, resulting in a decreased number of SEPA-1 aggregates in early stage mutant embryos compared to wild-type embryos at the same stage (H. Zhang, unpublished data).

Cautionary notes: SEPA-1 exhibits a dynamic pattern during embryogenesis, so embryos at the same developmental stages
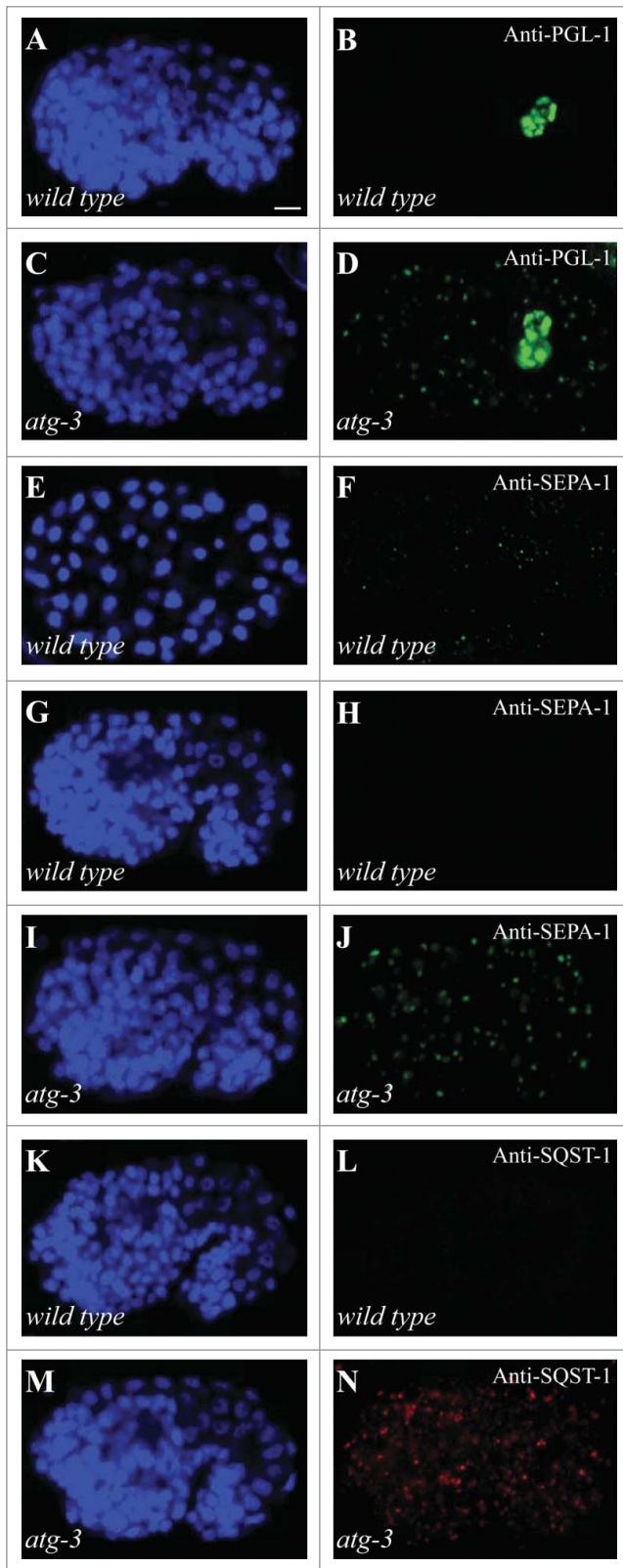

Figure 4. Various protein aggregates are degraded by autophagy during embryogenesis. ((**A**)**and B**) PGL-1 granules are restricted to germ precursor cells Z2 and Z3 in wild-type embryos. ((**C**)**and D**) PGL-1 granules accumulate in somatic cells in *atg-3* mutant embryos. ((**E**)**and F**) SEPA-1 forms spherical aggregates at the ~100 cell stage in wild-type embryos. ((**G**)**and H**) SEPA-1 aggregates disappear in wild-type comma stage embryos. ((**I**)**and J**) SEPA-1 aggregates accumulate in *atg-3* mutant embryos throughout embryogenesis. ((**K**)**and L**) No SQST-1 aggregates are detected in wild-type embryos. ((**M**)**and N**) SQST-1 accumulates into numerous aggregates in *atg-3* mutant embryos. (**A, C, E, G, I, K, and M**) DAPI images of the animals shown in (**B, D, F, H, J, L, and N**), respectively. Scale bar: 5 μm (**A-N**).

should be used for analysis. SEPA-1 is zygotically synthesized and is absent in germline cells.[7] Thus, unlike P granules, SEPA-1 does not accumulate in somatic-to-germ cell fate transformation mutants. To determine levels of SEPA-1 in an immunoblotting assay, extracts of late-stage embryos should be used, as a large number of SEPA-1 aggregates are present in early-stage embryos.

The receptor protein SQST-1

SQST-1 exhibits sequence similarity to mammalian SQSTM1 and is also degraded by autophagy.[4] Unlike SEPA-1, which forms aggregates in early stage embryos, SQST-1 is weakly expressed and diffusely localized in the cytoplasm throughout embryogenesis (**Fig. 4K and L**).[4] Blocking autophagy increases the levels of SQST-1 and also results in accumulation of a large number of SQST-1 aggregates (**Fig. 4M and N**).[4] In autophagy mutants, SQST-1 aggregates are evident from the 64- to ~100-cell stages onward and persist throughout embryogenesis.[4] SQST-1::GFP exhibits the same expression pattern as endogenous SQST-1 as detected by the anti-SQST-1 antibody. [4]

In different autophagy mutants, SQST-1 aggregates and PGL granules exhibit distinct morphologies and distribution patterns. In mutants with defects in the 2 ubiquitin-like conjugation systems, the UNC-51-EPG-1-EPG-9 (Atg1) complex and the PtdIns3K (Vps34) complex, SQST-1 aggregates are spherical and dispersed in the cytoplasm, and are separable from PGL granules.[6] In *epg-3, -4, -6,* and *atg-2* mutants, which block autophagosome formation, SQST-1 aggregates and PGL granules are irregular in shape and form cluster-like structures.[4,5.] These distinct phenotypes can be used for genetic epistasis analysis.

Accumulation of SQST-1 aggregates and PGL granules in hypomorphic autophagy mutants can be suppressed by elevated autophagy. For example, overexpression of EPG-6 suppresses the accumulation of PGL granules in *atg-3* hypomorphic mutants.[5] This assay, together with monitoring the number of LGG-1 puncta and SEPA-1 removal, can be applied to determine whether autophagy activity is elevated during embryogenesis.

Cautionary notes: SQST-1 accumulates in dead embryos with abnormal morphogenesis. Properly developed embryos should be used to examine the expression pattern of SQST-1. Embryos at the same developmental stage should be used for analysis of suppression of protein aggregate accumulation in hypomorphic autophagy mutants, as the number of protein aggregates varies during embryogenesis.

Other protein aggregates

In *C. elegans*, a group of coiled-coil domain-containing proteins, including C35E7.6, ZK1053.4, T04D3.1, T04D3.2, and F44F1.6, show limited sequence similarity to SEPA-1. These proteins are also degraded by autophagy during embryogenesis.[7] In loss of autophagy activity mutants, levels of these proteins are dramatically increased and accumulate into aggregates.[4,5,7,15-17] ZK1053.4 and C35E7.6 colocalize with SQST-1 aggregates, while T04D3.1, T04D3.2 and F44F1.6 aggregates are distinct from SQST-1 aggregates in autophagy mutants.[35] Thus, loss of autophagy activity causes accumulation of different types of protein aggregates during *C. elegans* embryogenesis.

Cautionary notes: Loss-of-function of essential autophagy genes causes a defect in degradation of PGL granules, SQST-1 aggregates and other protein aggregates as described above, but some factors confer selectivity on autophagic degradation, and loss of function of these genes results in a defect in degradation of certain types of protein aggregates. For example, mutations in *epg-2* cause a defect in removal of PGL granules, but have no effect on degradation of SQST-1, whereas mutations in *epg-7* cause a defect in degradation of SQST-1 but not PGL granules.[4,35] EPG-2 and EPG-7 function as scaffold proteins that link protein aggregates with the autophagic machinery.[4,35] Thus, different substrates, including PGL granules and SQST-1 aggregates, should be examined to determine whether a gene is generally required for autophagy.

Selective removal of paternal mitochondria and MOs during embryogenesis

Paternal mitochondria and membranous organelles (MOs) are engulfed by autophagosomes soon after fertilization and degraded by the 8-cell stage.[29,30] This type of autophagy has been termed allogeneic (non-self) organelle autophagy, or allophagy. Allophagy is required for complete elimination of paternal mitochondrial DNA from embryos in *C. elegans*. Ubiquitination has been observed on MOs preceding autophagosome formation, although it has not been determined whether this ubiquitination is functionally required for allophagy. In contrast to MOs, no obvious ubiquitination has been observed in paternal mitochondria.[29,30] Degradation of paternal organelles is inhibited by mutations or RNAi of core autophagy genes such as *unc-51*, *atg-5*, *atg-7*, *atg-18*, and *lgg-1*, and paternal organelles remain in 32-cell stage embryos or later stages as small puncta. In *lgg-1* and *atg-18* knockout mutants, paternal mitochondria are detectable even in L1 larvae. The number of paternal mitochondria does not increase in autophagy mutants, suggesting that they lose their ability to proliferate. It is difficult to convincingly detect paternally-inherited mitochondria in L2 or later-stage animals because the body mass expansion dilutes the signal.

To visualize paternal mitochondria, males can be stained with MitoTracker Red CMXRos and crossed with unstained hermaphrodites.[29,30] Alternatively, transgenic worms expressing mitochondria-targeted GFP fusion proteins (HSP-6::GFP or ANT-1.1::GFP) under control of a sperm-specific promoter can be used.[29,30] MOs are detected using the monoclonal antibody 1CB4 or SP56 that specifically stains MOs.[36,37] The autophagic degradation of paternal mitochondria can be examined by monitoring the degradation of paternal mitochondrial DNA (mtDNA) using a PCR-based method. In particular, a large deletion mutant of mtDNA (*uaDf5*) can be used to detect male mtDNA.[38] *uaDf5* is stably maintained in a heteroplasmic state with the wild-type mtDNA (*uaDf5*/+; approximately 60% of mtDNA harbors the deletion in each individual) and can be distinguished from wild-type mtDNA by using PCR. When *uaDf5*/+ males are crossed with hermaphrodites, *uaDf5* is not normally transmitted to the next generation because of autophagy-dependent degradation of paternal mitochondria. However, in the

autophagy mutant background, paternal *uaDf5* is detectable in the F1 embryos or larvae.

Cautionary notes: To detect paternal organelles or mtDNA in F1 larvae, hermaphrodites and males derived from the same autophagy mutants should be used. When males and hermaphrodites are crossed, autophagosome formation at the 1-cell stage depends on the autophagic activity of oocytes. However, the genotype of the males could affect the results. When wild-type males are crossed to autophagy-defective mutant hermaphrodites, autophagy is not induced in the F1 1-cell stage embryos, but is rather activated in later-stage embryos because of the paternally provided wild-type allele. In this situation, the degradation of paternal organelles is delayed, but eventually occurs in late-stage embryos, probably because of nonselective autophagic turnover of cytoplasmic components or normal allophagy that occurs later or more slowly once the paternal genome is expressed.

Monitoring Autophagy at Post-Embryonic Stages

After hatching, *C. elegans* go through 4 larval stages (called L1-L4), separated by molting, before developing into sexually mature adults. Unlike embryos, larvae and adult animals rely on external nutrients for development. In larvae and adult animals, hypodermis, seam cells and intestinal cells have so far been extensively characterized for autophagy phenotypes.

LGG-1 puncta and levels of LGG-1

In well-fed, wild-type animals, GFP::LGG-1 is diffusely localized in various tissues at larval and adult stages (**Fig. 5A,B,D and E**). Upon starvation, GFP::LGG-1 puncta increase in hypodermis, seam cells, and intestinal cells, representing an increase in autophagy (**Fig. 5C and F**). Accumulation of GFP::LGG-1 puncta can also result from a block in autophagy flux. Numerous GFP::LGG-1 puncta accumulate in *epg-6* and *epg-5* mutants, in which autophagy is blocked at the formation of autophagosomes and degradative autolysosomes, respectively (**Fig. 5G**). A large number of GFP::LGG-1 puncta accumulate in multiple tissues in *atg-3* mutants at the L1 larval stage (**Fig. 5H**), but largely disappear at late larval stages (**Fig. 5I**). Similar to the embryo, both an increase or decrease in autophagy can cause increased levels of LGG-1-II in an immunoblotting assay.[39,40] Thus, in addition to formation of GFP::LGG-1 puncta and levels of LGG-1-II, other assays, including degradation of substrates such as SQST-1, should be examined to determine autophagic flux.[39,40] *C. elegans* are enclosed by a cuticular structure that is impermeable to antibodies. For immunostaining assays, larvae and adult animals can be cut in the middle and then stained with anti-LGG-1.[39,40] Compared to immunostaining with anti-LGG-1, the GFP::LGG-1 reporter is much more convenient for analyzing the expression pattern of LGG-1.

When an increase in GFP::LGG-1 puncta is observed, this condition could be further tested in autophagy-compromised animals such as autophagy mutants or with RNAi-mediated autophagy inhibition. While use of RNAi is very powerful for inhibition of autophagy in *C. elegans*, one generation of autophagy RNAi is usually not sufficient to see effects on the GFP::LGG-1 reporter in larvae or in adults.[12] However, acute inhibition of autophagy, specifically in adult animals, can be done using the autophagy inhibitor bafilomycin A$_1$,[41,42] which is commonly used in mammalian systems to inhibit acidification of autolysosomes.[21] Bafilomycin A$_1$ can be injected into adult wild-type worms and an increase in the number of autophagosomes can be observed in as few as 2 h post-injection as determined by an increase in GFP::LGG-1 puncta in the seam cells of wild-type animals, consistent with a block in autophagy[91] (**Fig. 6A and B**).

Cautionary notes: Formation of GFP::LGG-1 puncta is sensitive to a variety of stresses, including starvation and contamination. The GFP::LGG-1 reporter is also sensitive to the type of anesthetics used to mount the transgenic animals; very few LGG-1-puncta are observed in animals mounted in 0.1% NaN$_3$, whereas levamisole or tetramisole hydrochloride both cause noticeable levels of puncta within 5–10 min of mounting the animals (**Fig. 7A–F**). When scoring GFP::LGG-1-positive puncta in the intestine of adult animals, autofluoresence is an issue. Use of confocal microscopy to restrict the excitation and emission wavelengths can alleviate this problem to some degree.

As noted above, an increase in the number of GFP::LGG-1 puncta may result from either elevated or impaired autophagic flux.[39,40] Therefore, the formation of GFP::LGG-1 puncta should be carefully interpreted and autophagy in larvae or adults should be examined by additional methods, including bafilomycin A$_1$ treatment, monitoring the degradation of autophagy substrates and electron microscopy.

Autophagy substrates in the intestine and hypodermal cells

In wild-type animals, SQST-1::GFP is weakly expressed at the larval and adult stages (**Fig. 8A and B**). In autophagy mutants, SQST-1::GFP accumulates into a large number of aggregates in multiple tissues, including the epidermis, neurons and intestine (**Fig. 8C and D**). Autophagy activity is induced in response to a variety of stresses. In *epg-7* mutants, accumulation of SQST-1::GFP in larvae can be suppressed by the inactivation of LET-363/TOR signaling or by starvation.[35] Levels of SQST-1::GFP can also be determined in an immunoblotting assay.[40]

W07G4.5::GFP, a nematode-specific protein, is also selectively removed by autophagy at post-embryonic stages.[35] W07G4.5::GFP is mainly expressed in the intestinal cells and forms aggregates that are localized in the cytoplasm and also in the nuclei at larval stages.[35] In autophagy mutants, W07G4.5::GFP is present at dramatically elevated levels and forms more aggregates in the intestine.[35] W07G4.5::GFP aggregates dramatically decrease upon induction of autophagy in response to stimuli such as starvation or inactivation of LET-363/TOR signaling.[35,40]

Cautionary notes: Accumulation of SQST-1::GFP may also result from a defect in autophagy-unrelated processes. For example, SQST-1::GFP can label damaged organelles or protein aggregates (see the section below on *rpl-43*) that do not result from impaired autophagy activity. Thus, additional assays, such as GFP::LGG-1 puncta and levels of LGG-1-II, should be analyzed to examine autophagy.
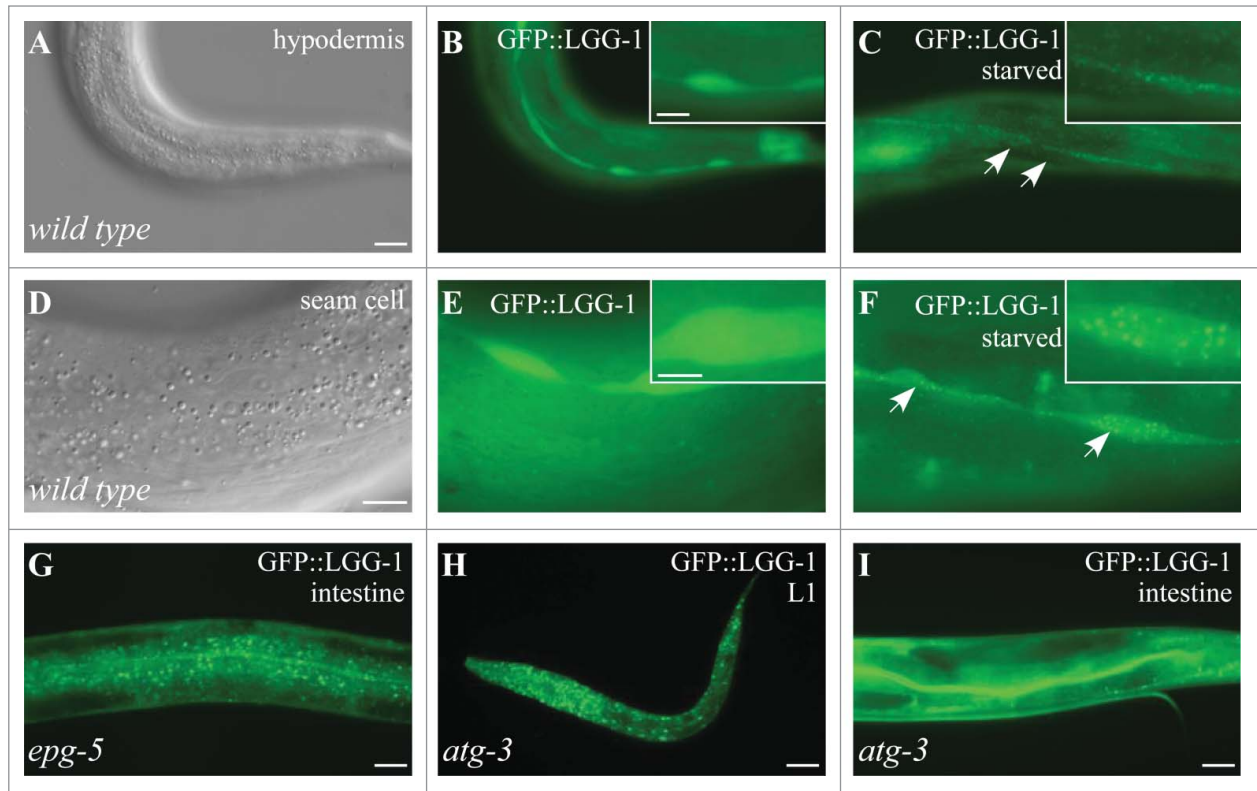
Figure 5. GFP::LGG-1 pattern at post-embryonic stages. (**A and B**) GFP::LGG-1 is diffusely localized in the hypodermis of wild-type animals. (**A**) DIC image of the animal shown in (**B**). (**C**) GFP::LGG-1 forms numerous small punctate structures in the hypodermis after the animals are starved for 4 h. (**D and E**) GFP::LGG-1 is diffusely localized in seam cells of wild-type animals. (**D**) DIC image of the animal shown in (**E**). (**F**) GFP::LGG-1 forms many small punctate structures in the seam cells after the animals are starved for 4 h. Inserts show magnified views. (**G**) Numerous GFP::LGG-1 punctate structures are observed in the intestine of *epg-5* mutants. L4 larvae are shown in (**A-G**). (**H and I**) A large number of GFP::LGG-1 puncta accumulate in *atg-3* mutants at the L1 larval stage (**H**), but largely disappear at late larval stage (**I**). Scale bars: 20 μm (**A–C, G-I**); 10 μm (**D–F**); 10 μm (inserts in (**B and C**); 5 μm (inserts in (**E and F**).

SQST-1::GFP aggregates in *epg-7* mutant larvae and also W07G4.5 aggregates in wild-type larvae are removed by autophagy induced by a variety of stresses. Therefore, all strains need to grow under nutrient-rich and contamination-free conditions. The number of aggregates also varies at different developmental stages; therefore, animals at the same larval/adult stage should be compared. As some mutations or treatments could delay growth, animals should be synchronized by developmental, not chronological, age.
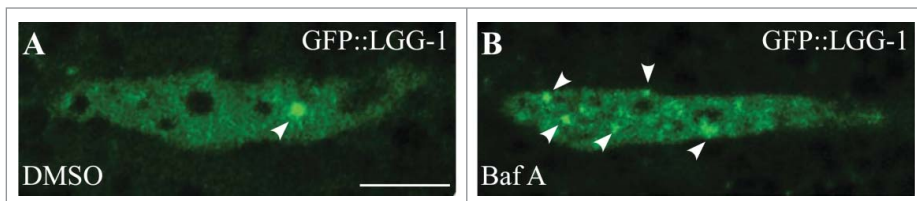

Figure 6. Bafilomycin A$_1$ treatment increases GFP::LGG-1 puncta in seam cells of adult animals. (**A**) A few GFP::LGG-1 puncta form in seam cells in DMSO-treated wild-type day 1 adult animals. (**B**) The number of GFP::LGG-1 puncta dramatically increases after bafilomycin A$_1$ (Baf A) treatment for 2 h in wild-type day 1 adult animals. Arrows point to puncta. Scale bar: 5 μm.

Suppression of SQST-1 aggregates in *rpl-43* mutants

rpl-43 encodes the 60S ribosomal protein L37, and detection of SQST-1 aggregates in *rpl-43* mutants can be another assay to determine autophagy activity. *rpl-43(bp399)* hypomorphic mutants show accumulation of SQST-1::GFP aggregates (**Fig. 9A and B**).[40] Unlike in autophagy mutants, SQST-1 aggregates are restricted to intestinal cells in *rpl-43(bp399)* mutants.[40] Loss-of-function of *rpl-43* does not cause a defect in the degradation of other autophagic substrates, including C35E7.6, ZK1053.4, SEPA-1, PGL-1, and PGL-3.[40] Thus, *rpl-43* is not an essential autophagy gene. SQST-1 aggregates in *rpl-43* intestinal cells are removed by elevated autophagy, induced by starvation, inactivation of LET-363/TOR signaling, DAF-2/IGF1R (insulin-like growth factor 1 receptor) signaling, SMA-6-MAB-31 (Sma-Mab) TGFB signaling and LIN-35/RB1 signaling, and also by ER stress and mitochondrial stress (**Fig. 9C–F**).[40]

Cautionary notes: The number of intestinal SQST-1 aggregates in *rpl-43* mutants is very sensitive to a variety of

stresses. For example, accumulation of SQST-1 aggregates in *rpl-43* mutants, is suppressed by high temperature (25°C), starvation, or bacterial contamination. *rpl-43* mutants must be grown under well-fed, noncontaminated conditions at 20°C. Partial loss of function of some essential autophagy genes, including components of the ESCRT complex (*hgrs-1, vps-37*) and subunits of the NAC complex (*icd-1* and *icd-2*), also suppress the *rpl-43* phenotype.[39,40] This is probably because partial inactivation of these genes poses a stress on the animal that further induces autophagy activity.

Transcriptional regulation of autophagy

Autophagy gene expression can easily be measured in adult animals using standard quantitative PCR methods. For example, in response to inhibition of LET-363/TOR signaling or dietary restriction, an increase in mRNA levels of multiple autophagy genes (e.g., *lgg-1* and *atg-18*) is observed.[43,44] LET-363/TOR regulates autophagy gene expression, in part via the helix-loop-helix transcription factor HLH-30, an ortholog of mammalian TFEB.[43,45] In response to LET-363/TOR inhibition, HLH-30/TFEB translocates to the nucleus in the intestine of the adult animal, as visualized by a HLH-30::GFP reporter (**Fig. 10A and B**). As such, this transgenic strain can be used as an indirect assay to study autophagy induction.

Cautionary notes: As for quantitative PCR experiments in general, it is important to normalize gene expression to multiple control genes (e.g.,, *act-1, cyn-1, ama-1, nhr-23, pmp-3,* and *cdc-42*). HLH-30 nuclear translocation needs to be performed while carefully controlling for temperature because small changes in temperature will cause HLH-30 nuclear translocation.[43] Note also that since HLH-30/TFEB regulates additional genes besides autophagy genes,[45,46] it is possible that HLH-30 has autophagy-independent outputs.

Transmission electron microscopy

Unlike in yeast and mammalian systems, TEM has been relatively underutilized in *C. elegans* autophagy research.[23,47] In principle, TEM (including immuno-electron microscopy) can be applied to visualize all forms of autophagy in all developmental and physiological processes in *C. elegans*. Phagophores,
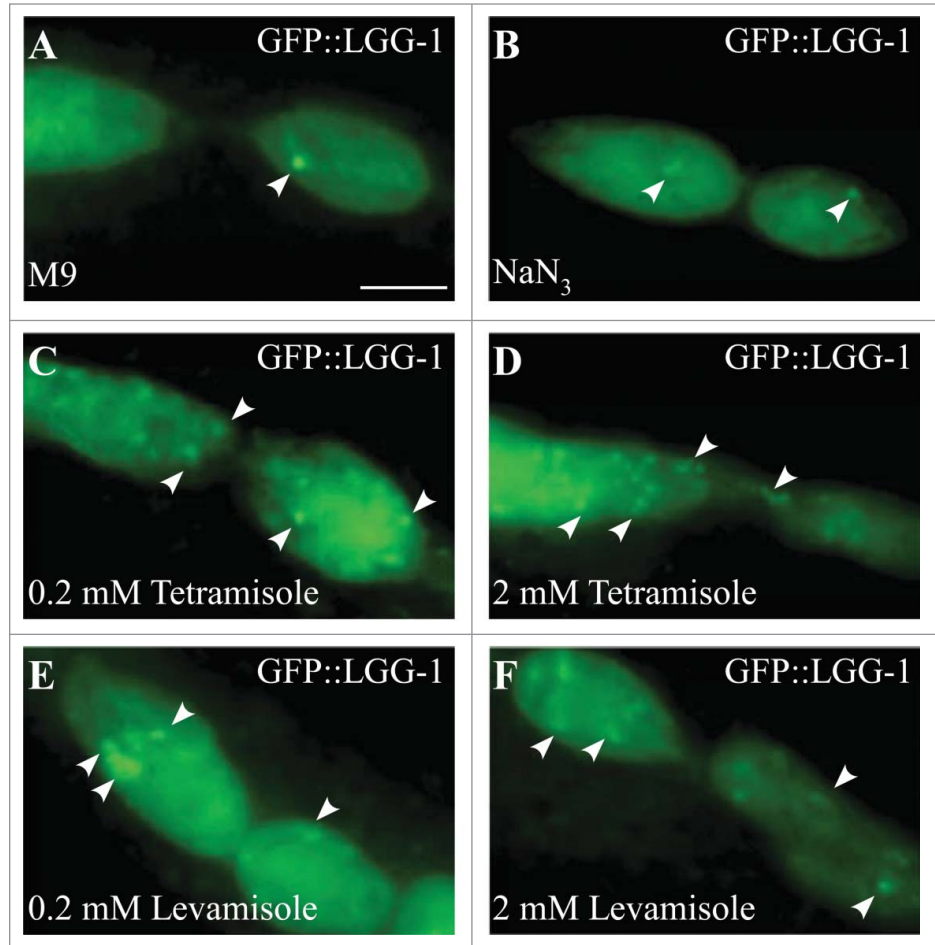

Figure 7. GFP::LGG-1 pattern in L3 larva using different mounting methods. (**A**) GFP::LGG-1 is largely diffuse in seam cells of L3 larvae mounted with M9 medium on a 2% agarose pad. These animals are not paralyzed. (**B**) GFP::LGG-1 is largely diffuse in seam cells of fully anesthetized L3 larvae mounted in a final concentration of 0.1 % (w/v; ~150 mM) NaN$_3$ in M9 medium on a 2% agarose pad with the same concentration of NaN$_3$. (**C–D**) GFP::LGG-1 forms many different-sized punctate structures (arrows) in the seam cells (and other tissues) of fully anesthetized L3 larvae mounted in a final concentration of 0.2 mM (**C**), or 2 mM (**D**) tetramisole in M9 medium on a 2% agarose pad. Punctate structures start appearing 5 min after mounting. (**E–F**) GFP::LGG-1 forms many different-sized punctate structures (arrows) in the seam cells (and other tissues) of fully anesthetized LC3 larvae mounted in a final concentration of 0.2 mM (**C**) or 2 mM (**D**) levamisole in M9 medium on a 2% agarose pad. Punctate structures start appearing 5 min after mounting. Scale bar: 5 μm.

autophagosomes, and autolysosomes represent 3 main consecutive stages of the autophagic process (**Fig. 11A–C**). In *C. elegans*, phagophores are extremely rare under control conditions; only a single one was identified in sections from several hundred worms.[47] In contrast, autophagosomes and autolysosomes are far more frequent, both compartments occupying 10^{-3}–10^{-1}% of the cytoplasmic volume, similar to mammalian cells.[47–49] Large, complex, and darker appearing autolysosomes may also occur infrequently; however, in dauers and starved worms they are found in high numbers (**Fig. 11D**). The changes in autophagic structures and numbers may reflect elevated or impaired autophagy. If major increases occur in the quantity of the 3 basic compartments, but their relative cytoplasmic ratios do not show a significant shift, autophagic flux appears to be increased, such as
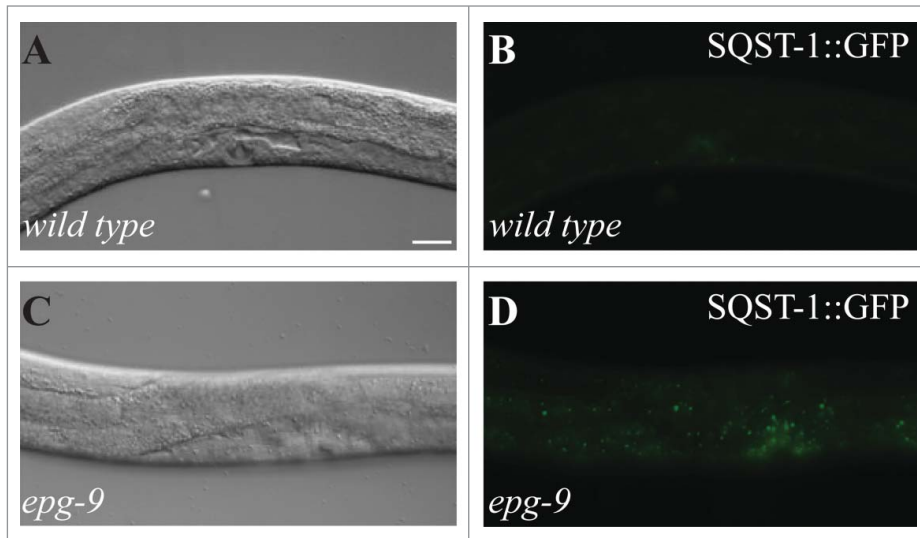
Figure 8. Expression of SQST-1 aggregates at larval stages. (**A and B**) SQST-1::GFP is weakly expressed in wild-type L4 larvae. *bpIs151(sqst-1p:: sqst-1::gfp)* was used. (**C and D**) In *epg-9* mutants, SQST-1::GFP accumulates into aggregates in multiple tissues. (**A and C**) DAPI images of the animals shown in (**B and D**), respectively. Scale bar: 20 μm.

during starvation conditions. A similar expansion occurs in larval stages right after hatching or molting, probably as a consequence of unavoidable fasting during the embryonic or the lethargus

Figure 9. Accumulation of SQST-1 aggregates in the intestine in *rpl-43* mutants. (**A and B**) SQST-1::GFP accumulates into a large number of aggregates in the intestine in *rpl-43* mutant L4 larvae. (**C-F**) Accumulation of SQST-1 aggregates in *rpl-43* mutant L4 larvae is suppressed by elevated autophagy activity induced by starvation (**C and D**) or by *lin-35* inactivation (**E and F**). (**A, C, and E**) DIC images of the animals shown in (**B, D, and F**), respectively. Scale bar: 20 μm (**A–F**).

phase.[47] The relative increase in autophagosome quantity may be the consequence of diminished fusion with endosomes and lysosomes. Conversely, the preferential expansion of darker autolysosome compartments may be the consequence of impaired lysosomal digestion.[49]

TEM analysis of autophagic structures has also been performed in several autophagy mutants. *unc-51(e369)* mutants contain large complex "myelinated" autophagic structures (**Fig. 11E**).[47] In *epg-3*, *epg-4*, *epg-6*, *atg-2*, and *atg-18* mutants, phagophores are far more abundant than in control cells since autophagosome formation is inhibited.[4,5] In *epg-4* and *atg-2* mutants, finely layered, possibly phospholipid, structures associated with rough endoplasmic reticulum (RER) and phagophores are observed. Furthermore, in *epg-4* mutants, large areas of RER are devoid of ribosomes while their inner space becomes empty like that of the phagophore.[4] These observations indicate the involvement of these genes in the formation of the early phagophore and its further progress to create autophagosomes.

Cautionary notes: The application of TEM to autophagy studies is relatively time consuming and demands high-level technical expertise in the recognition of subcellular structures. Although there are pitfalls in detecting and identifying all 3 major compartments,[23,47] a major problem specific to *C. elegans* is the presence of many types of membrane-bound secretory and protein granules that may resemble autolysosomes and are especially numerous in intestinal cells (**Fig. 11F–H**). A sequential step-by-step analysis of the deterioration of the autophagic contents during the degradation process may help to overcome this identification difficulty. Only structures that follow the delineated morphological features found by a serial analysis can be determined as autophagic in origin.[23] The size of each autophagic subcompartment (i.e., phagophore, autophagosome, autolysosome) is determined by the ratio between the rate of autophagy induction and the rate of autophagic degradation. Therefore, the growth in size of a
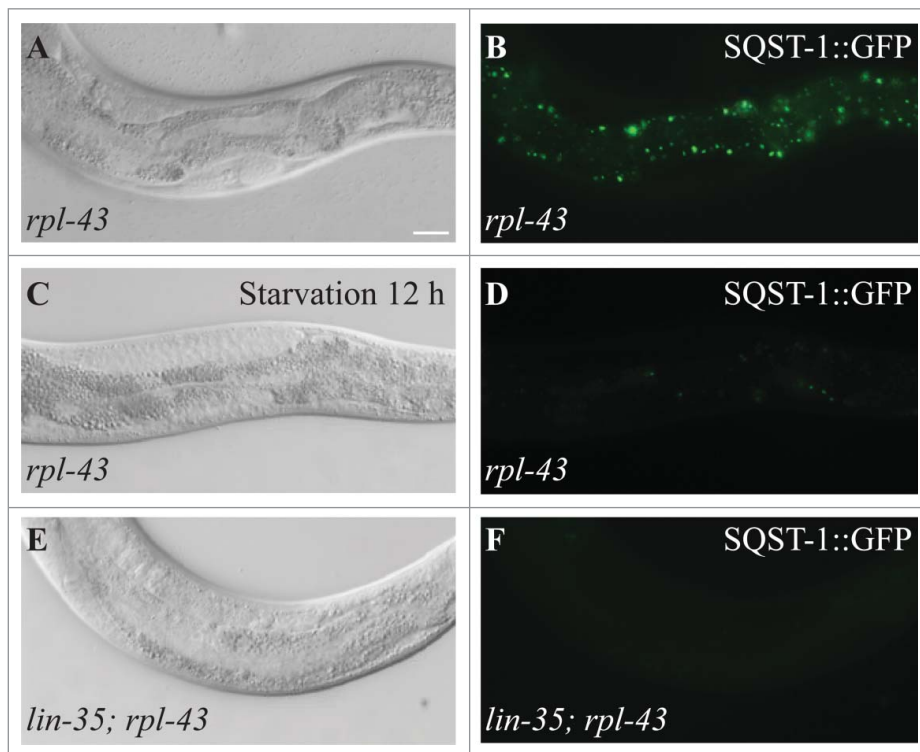
subcompartment may come from the relative increase of the rate of autophagy induction and/or the relative decrease in autophagic degradation.

Biological Processes Linked to Autophagy in *C. elegans*

Autophagy plays critical roles in a number of physiological processes occurring during development and in adult *C. elegans*. In addition to the removal of a variety of protein substrates and paternal mitochondria following fertilization, autophagy also regulates survival of L1 larvae, dauer development, aging, cell fate specification, cell death, and cell corpse removal. However, defects in these processes can also result from loss of function of genes independent of autophagy activity. These phenotypes can therefore only provide supporting evidence for autophagy regulation, and should not be used as an indicator of autophagic flux during development.

L1 larvae survival

Under food deprivation conditions, newly hatched larvae arrest at the L1 (first larval) stage and maintain viability for 1–2 weeks. Autophagy, which generates survival materials such as macromolecules and ATP, regulates L1 survival in the absence of food. Starvation activates autophagy, possibly through the

Figure 10. HLH-30::GFP translocates to the nucleus upon LET-363/TOR inactivation in adult animals. (**A**) HLH-30::GFP shows diffuse localization in the cytoplasm in the intestine of day 1 animals. (**B**) HLH-30::GFP translocates to the nucleus following whole-life *let-363/TOR* RNAi treatment. Scale bar: 300 μm.

muscarinic acetylcholine signaling pathway.[28,50] Reduced autophagy activity caused by loss of function of essential autophagy genes decreases the L1 survival rate during starvation.[4,5,15-17,24,28] An excessive level of autophagy also shortens L1 survival. In *gpb-2* mutants, in which muscarinic acetylcholine signaling is overactivated, starvation induces excessive autophagy, which in turn exerts a prodeath effect.[28] Thus, decreased survival of L1 larvae could be attributed to either insufficient or excessive levels of autophagy.

Cautionary notes: Embryos should be washed completely to remove any bacteria before suspension in M9 buffer for analysis. The total number of L1 larvae is counted after the animals are seeded on the plates at time 0, and the viable animals are examined after growing them overnight.
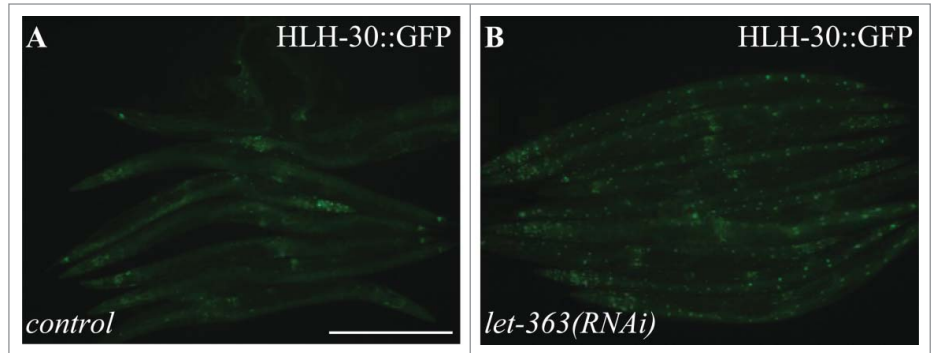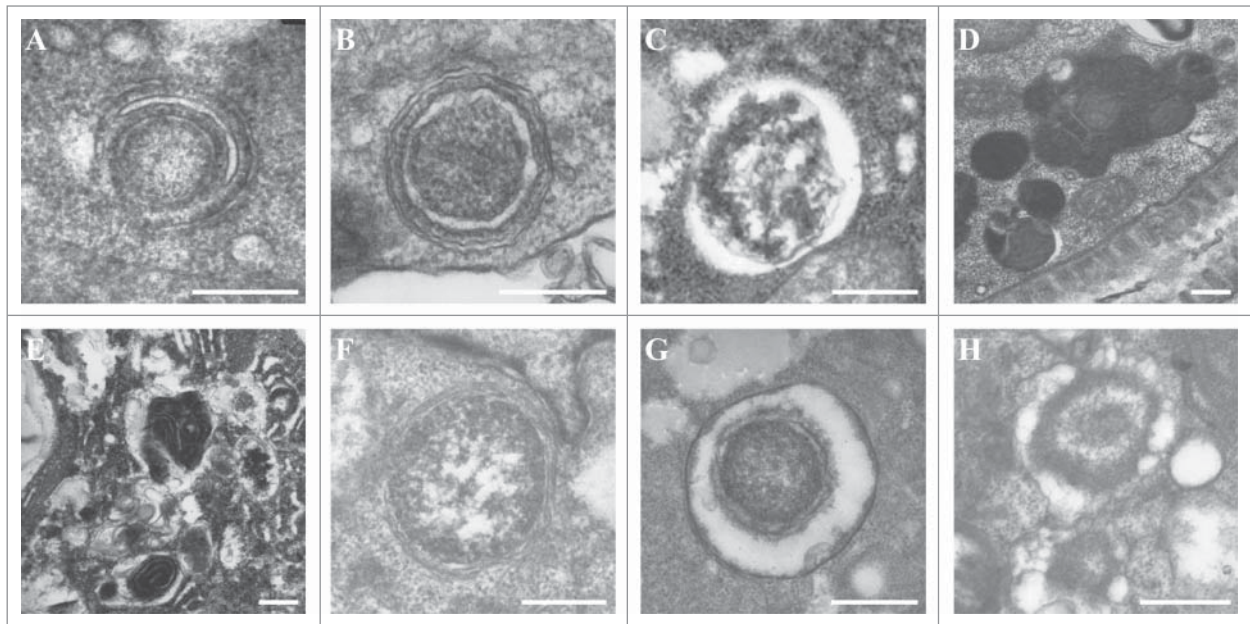
Figure 11. Electron microscopy images of autophagic structures in wild-type and autophagy mutants. (**A–D**) The 3 main autophagic structures (subcompartments): (**A**) phagophore; (**B**) autophagosome; (**C**) light-type, actively digesting autolysosome; (**D**) autolysosomes with dark undigested content—they may frequently have irregular shapes. (**E**) Complex myelinated autophagic structure in a hypodermal cell of an *unc-51(e361)* mutant. (**F–H**) Three types of secretory vacuoles, which are similar to autolysosomes. Scale bars: 500 nm.

Dauer formation

In response to harsh environmental conditions, such as low food abundance, high temperature, and/or overcrowding, *C. elegans* larvae arrest in the second molt as dauer larvae. Dauer larvae undergo morphological and metabolic changes that allow them to survive harsh environmental conditions, such as radial constriction of the body and constriction of the pharynx, lack of pharyngeal pumping, closure of oral cavities, and the formation of a specialized cuticle with lateral ridges, referred to as dauer alae.[51,52] Thus, dauer animals are adapted to resist metabolic and environmental stresses. They are also long-lived, as they can live as dauers for months.[53] Several evolutionarily conserved pathways regulate the decision to enter dauer development, such as those involving guanylyl cyclase, TGFB (transforming growth factor), and INS/IGF1 (insulin/insulin-like growth factor 1 [somatomedin C]), and a steroid hormone signaling pathway.[54] Mutants in these pathways, for example loss-of-function mutants in *daf-2*, are constitutive dauers at the restrictive temperature, even in the presence of food. *daf-2* constitutive dauers show an increase in GFP::LGG-1-positive puncta in hypodermal seam cells, as well as an increase in autophagosomes as visualized by TEM.[10] These increases are interpreted as an increase in autophagy activity, since autophagy genes are required for many of the changes associated with the development of *daf-2* dauers and similarly for *daf-7*/TGFB dauers.[10]

Cautionary notes: Autophagy genes are required for normal development and their loss during development may cause pleiotropic defects. RNAi feeding to partially inactivate gene activity can be used to investigate the role of a gene in dauer formation.

Aging

The life span of animals is influenced by several conserved longevity paradigms, including dietary restriction, LET-363/TOR signaling, INS (insulin) signaling, and germline removal.[55] As a key catabolic process in degradation of damaged organelles and harmful protein aggregates, autophagy is thought to act downstream of these signaling pathways to modulate the life span of the organism.[56,57] Specifically, long-lived *C. elegans* mutants, such as *daf-2*, *let-363/TOR(RNAi)* mutants, dietary-restricted *eat-2* mutants, mitochondrial respiration *clk-1* mutants and germline-deficient *glp-1* mutants, exhibit increased levels of GFP::LGG-1 puncta as well as increased expression of at least some autophagy genes (e.g., *lgg-1*), and require autophagy genes (e.g.,, *lgg-1, bec-1,* and *atg-18*) for their life-span extension.[10–13,40,43,58,59] These observations imply that autophagy activity may be induced in these long-lived animals, contributing to their life-span extension. At least part of the induction of autophagy gene expression in such long-lived mutants is regulated by the transcription factor HLH-30/TFEB.[43,46]

Cautionary notes: All autophagy mutants analyzed to date are poorly developing, unhealthy and short-lived, likely since developmental processes are affected in these animals. For this reason, RNAi feeding after the L4 stage ("adult-only" RNAi) can be used to postdevelopmentally inactivate a particular autophagy gene to investigate its role specifically in the aging process.[57]

Necrotic death of touch neuron

The gain-of-function mutation in *mec-4*, which encodes a toxic ion-channel variant, causes necrosis-like degeneration of 6 touch receptor neurons. Touch receptor neurons can be visualized by P*mec-4*::GFP, a *gfp* reporter driven by the *mec-4* promoter. Loss-of-function of *epg-1*, *bec-1*, *lgg-1,* and *epg-6* reduces degeneration of touch neurons caused by *mec-4* gain-of-function mutations,[5,8,9,15,26] indicating that autophagy activity is essential for the necrotic death of touch neurons.

Cautionary notes: Touch neuron death is usually counted as the complete absence of the normal P*mec-4*::GFP fluorescent signal. Animals at the same developmental stage, such as L2 larvae, should be examined to determine the number of touch neurons marked by P*mec-4*::GFP.

ASEL/ASER cell fate specification

Autophagy degrades key components of the miRNA-induced silencing complex (RISC) and thus modulates miRNA-mediated gene silencing.[60–62] The *C. elegans* GW182 homolog AIN-1, a component of RISC, is selectively degraded by autophagy and colocalizes with SQST-1 in autophagy mutants.[62] Autophagy regulates various developmental processes controlled by miRNA. The *lsy-6* miRNA controls left-right asymmetry of the 2 taste receptor neurons ASE left (ASEL) and ASE right (ASER) by repressing *cog-1* expression in ASEL.[63] Loss of *lsy-6* activity causes the ASEL neuron to adopt the ASER fate. *lsy-6(ot150)* hypomorphic mutants display incomplete ASEL to ASER fate transformation.[64] The ASEL fate specification phenotype in *lsy-6(ot150)*, visualized by the P$_{lim-6}$::GFP reporter, is partially rescued by loss of autophagy activity, and is exacerbated by elevated autophagy activity caused for example by inactivation of LET-363/TOR signaling.[62]

Cautionary notes: The expression of the P$_{lim-6}$::GFP reporter in *lsy-6(ot150)* mutants shows some degree of variation under different growth conditions. A large number of larval animals at the same developmental stages should be examined and control animals should be included in parallel.

Regulation of cell corpse number during embryogenesis

During *C. elegans* embryogenesis, 113 somatic cells undergo programmed cell death.[65] Cell corpses are phagocytosed and removed by neighboring cells. The cell corpse-containing phagosome undergoes a series of maturation processes and eventually fuses with lysosomes for degradation. Mutations in autophagy genes acting at different steps of autophagosome formation and maturation cause an increased number of cell corpses.[66,67] Loss of autophagy activity does not affect the generation of cell corpses, but the maturation of cell corpse-containing phagosomes is impaired in autophagy mutants.[67]

Cautionary notes: The number of cell corpses varies in different embryonic stages. Embryos at the same developmental stage should be used for analysis.

Impaired γ-ray-induced germline cell death

During *C. elegans* oogenesis, a large proportion of germ cells at the meiotic pachytene stage undergo programmed cell death

Table 2. Methods to monitor autophagy activity in *C. elegans*.

	Method	Description[a]	Reagents and references
Embryonic stages	1. LGG-1 protein gel blotting	Accumulation of LGG-1-II can result from either elevated or impaired autophagy.	Anti-LGG-1 (ref. 4)
	2. LGG-1 immunostaining and GFP::LGG-1	Different autophagy mutants show distinct morphology and distribution patterns of LGG-1 puncta. LGG-1 puncta also accumulate in embryos with elevated autophagy.	*adIs2122(lgg-1p::gfp::lgg-1)* (ref. 10, 28),*dkIs398(pie-1p::gfp::lgg-1)* (ref. 29)
	3. LGG-2 immunostaining and GFP::LGG-2	GFP::LGG-2 puncta accumulate in some autophagy mutants.	Anti-LGG-2 (ref. 30), *pmcIs2(lgg-2p::gfp::lgg-2)* (ref. 30)
	4. Degradation of PGL-1 and PGL-3 in somatic cells	Accumulation of PGL-1 and PGL-3 in somatic cells indicates impaired autophagy. Accumulation of PGL granules in hypomorphic autophagy mutants can be suppressed by elevated autophagy.	*bnIs1(pie-1p::gfp::pgl-1)* (ref. 88), Anti-PGL-1 (ref. 89, 7), Anti-PGL-3 (ref. 90, 7), monoclonal K76 (ref. 89)
	5. Degradation of SEPA-1	SEPA-1 granules, detected by anti-SEPA-1 or SEPA-1::GFP, accumulate in late stage embryos when autophagy is inhibited. The number of SEPA-1 granules decreases in early stage embryos when autophagy is induced.	Anti-SEPA-1 (ref. 7), *bpIs131(sepa-1p::sepa-1::gfp)* (ref. 7)
	6. SQST-1 turnover	SQST-1 aggregates, detected by anti-SQST-1 or SQST-1::GFP, accumulate when autophagy is inhibited. The amount of SQST-1 increases when autophagy is inhibited.	Anti-SQST-1 (ref. 4), *bpIs151(sqst-1p::sqst-1::gfp)* (ref. 4)
	7. Degradation of SEPA-1 family members	Autophagy inhibition causes accumulation of aggregates formed by SEPA-1 family members.	*bpIs132(c35e7.6p::c35e7.6::gfp), bpIs128(zk1053.4p::zk1053.4::gfp), bpIs129(t04d3.1p::t04d3.1::gfp), bpIs126(f44f1.6p::f44f1.6::gfp), bpIs120(zk1053.3p::zk1053.3::gfp)* (ref. 7, 16, 35)
	8. Paternal mitochondria and organelle removal	Autophagy inhibition leads to persistence of paternal mitochondria and MOs in embryos beyond the 8-cell stage.	Mitochondria: *dkIs623(spe-11p::hsp-6::gfp)* (ref. 29), *pmcIs1(ant-1.1p::ant-1.1::GFP)* (ref. 30), *uaDf5* (ref. 38). MOs: monoclonal 1CB4 (ref. 36), SP56 (ref. 37)
Larval stages	1. LGG-1 western blotting	Accumulation of LGG-1-II can result from either elevated or impaired autophagy.	Anti-LGG-1 (ref. 4)
	2. GFP::LGG-1	GFP::LGG-1 puncta accumulate in multiple tissues, including seam cells and intestinal cells, upon induction of autophagy, but also in mutants of autophagy genes acting at distinct steps of the autophagy pathway. Autophagy can be blocked in adult worms by bafilomycinA1 injection.	*adIs2122(lgg-1p::gfp::lgg-1)* (ref. 10, 28)
	3. GFP::LGG-2	GFP::LGG-2 puncta accumulate in multiple tissues, including seam cells and neurons.	*ppEx108(lgg-2p::gfp::lgg-2)* (ref. 24)
	4. SQST-1::GFP turnover	SQST-1::GFP accumulates into a large number of aggregates in multiple tissues when autophagy is inhibited. Accumulation of SQST-1::GFP aggregates in hypomorphic autophagy mutants is suppressed and the amount of SQST-1::GFP is reduced upon autophagy induction.	*bpIs151(sqst-1p::sqst-1::gfp)* (ref. 4).
	5. W07G4.5::GFP turnover	W07G4.5::GFP aggregates accumulate in the intestine when autophagy is impaired. When autophagy is induced, W07G4.5::GFP aggregates in wild-type animals or hypomorphic autophagy mutants decrease and the amount of W07G4.5::GFP is reduced.	*bpIs239(w07g4.5p::w07g4.5::gfp)* (ref. 35)
	6. SQST-1::GFP in *rpl-43* mutants	Suppression of SQST-1 aggregates in *rpl-43* mutant intestinal cells suggests elevated autophagy.	*bpIs151(sqst-1p::sqst-1::gfp)* (ref. 4)
	6. Transcriptional regulation		*sqIs19(hlh-30p::hlh-30::gfp)* (ref. 43)

Table 2. Methods to monitor autophagy activity in *C. elegans*. *(Continued)*

Method	Description[a]	Reagents and references
	qRT-PCR to determine expression of various autophagy genes. HLH-30/TFEB nuclear translocation leads to upregulation of autophagy genes.	
7. Transmission electron microscopy	Monitor autophagic structures, number and volume.	

[a]Quantification of the number of punctate structures can be performed by manual live counting at the microscope, manual counting of pictures, or automatic counting, e.g., by Imaris software when using confocal microscopy. Immunoblotting analysis can be performed to detect protein levels when weak phenotypic effects are observed.

and act as nurse cells to provide cytoplasmic components for maturing oocytes.[68] DNA damage (induced for example by γ-ray irradiation) or various environmental stresses (e.g., oxidative, heat and osmotic stresses) also trigger the death program in meiotic pachytene-stage germ cells.[69,70] In autophagy mutants, fewer germ cells execute the death program upon γ-ray treatment.[71] Autophagy also contributes to physiological germ-cell death and post-embryonic cell death in ventral cord neurons when *ced-3* caspase activity is partially compromised.[71]

Cautionary notes: Animals at the same developmental stage should be used for treatment and the number of cell corpses needs to be analyzed at the same time after the treatment. For γ-ray irradiation, L4 worms are aged for 12 h before being treated with 120 Gy γ-rays (Gammacell 1000). Germ cell corpses are quantified 24 h post-irradiation.

Degradation of lipid droplets

Lipophagy, autophagy-mediated degradation of lipid droplets, regulates fat storage in mammals and *C. elegans*.[46,72] Genetic evidence in worms has defined a number of lipolytic enzymes that are thought to mediate lipid mobilization through lipophagy. The genes *lipl-1* and *lipl-3*, which encode liposomal lipases, transcriptionally respond to autophagy-activating stimuli, including but not limited to starvation and inactivation of *let-363*/TOR signaling, *daf-2*/INS signaling, or Sma-Mab/TGFB signaling.[46] Similarly, the autophagy genes *lgg-1*, *lgg-2*, and *atg-16.2*, and the transcriptional regulator *hlh-30/Tfeb* are induced by autophagy-activating stimuli.[43,46] Therefore, quantitative PCR of *lipl-1*, *lipl-3*, and *lgg-1*, *lgg-2*, *atg-16.2*, and *hlh-30/Tfeb*, can be used as a proxy to assess lipophagy. This approach, in combination with quantification of cytoplasmic fat stores through fat staining such as with Oil Red O, can provide insight into the effect of genes or treatments on autophagy-mediated lipid mobilization.[73]

Cautionary notes: Fat levels change significantly during development. Therefore, animals at the same developmental age (vulva/germline development) and not chronological age (time from hatching or seeding) should be compared. The dynamic range for Oil Red O is optimal in young adults (6–24 h from L4 to adult molt at 20°C).

Xenophagy

A variety of bacterial pathogens, including the gram-negative bacterium *Salmonella enterica* serovar Typhimurium, can infect and kill *C. elegans*.[14,74-80] Xenophagy, the selective degradation of microorganisms through an autophagy-related mechanism,[3] engulfs and destroys invading *Salmonella* in several model systems including *C. elegans*.[14,81-83] Compared to wild-type *C. elegans*, autophagy-deficient worms die much faster and accumulate more *Salmonella* inside the body,[14] indicating that autophagy protects *C. elegans* against *Salmonella* infection by limiting the replication of the bacteria. Additionally, inhibition of the autophagy gene *bec-1* in the intestine but not in other tissues confers susceptibility to *Salmonella* infection, which indicates that autophagy acts cell-autonomously in the intestinal epithelial cells to defend against *Salmonella* infection in *C. elegans*.[84] Moreover, autophagy mediates the insulin-like signaling-regulated pathogen resistance in long-lived *daf-2* mutants with increased autophagy.[10,14] When *daf-2* mutant animals are treated with RNAi to silence the expression of autophagy genes, the increase in autophagy is suppressed to basal levels (as observed in wild-type animals) and the resistance of *daf-2* mutants to *Salmonella* infection is abrogated.[14] Thus, the decreased survival of *C. elegans* when infected by *Salmonella* results from reduced autophagy.

Cautionary notes: Life span is used to measure the influence of xenophagy on survival of *C. elegans* infected by *Salmonella*. The effect of autophagy deficiency on life-span may mask the killing effect of *Salmonella* infection. The level of autophagy deficiency, which can be modulated by altering the concentration of the RNAi inducer isopropylthio-β-galactoside/IPTG used in the RNAi feeding experiment,[14,84] should have no effect on life span. If it is impossible to achieve a desired partial suppression of autophagy, the Cox proportional-hazards model can be performed to compare survival times and estimate hazard (risk) ratios among control groups and *Salmonella*-infected groups to evaluate the effect of inhibition of xenophagy on survival of animals infected with *Salmonella*.[14]

Conclusion and Perspectives

Recent studies have established *C. elegans* as a powerful genetic model to delineate the autophagy pathway, such as through the

identification of metazoan-specific autophagy genes. Moreover, *C. elegans* has emerged as an excellent model system to reveal the functions of autophagy under physiological and stress conditions at the subcellular, tissue-specific, and organismal levels. For these studies, multiple assays for monitoring the autophagy process have been developed, yet it is important to note that each assay, summarized above, has its limitations and thus a combination of these assays (summarized in **Table 2**) should always be performed to make solid claims about autophagic activity. The development of additional assays, for example of tandem (i.e., mCherry::GFP) LGG-1 and LGG-2 reporters for expression in somatic tissues, as well as biochemical methods to assess autophagic turnover, will also be critical. With such an extended toolbox, the study of autophagy in different tissues at distinct developmental stages should aid in understanding whether components of the autophagic machinery are differentially employed and controlled by tissue-specific factors. Moreover, it will be interesting to learn how different environmental cues and signaling events during development and in adult animals are integrated into the autophagic machinery to control autophagy activity in a tissue- and temporal-specific manner. Undoubtedly, studies in *C. elegans* will provide valuable insights into the molecular mechanism of autophagy as well as how autophagy dysfunction leads to the development of a broad range of human age-related diseases, such as metabolic disorders and neurodegeneration.

Disclosure of Potential Conflicts of Interest

No potential conflicts of interest were disclosed.

References

1. Nakatogawa H, Suzuki K, Kamada Y, Ohsumi Y. Dynamics and diversity in autophagy mechanisms: lessons from yeast. Nat Rev Mol Cell Biol 2009; 10:458-67; PMID:19491929; http://dx.doi.org/10.1038/nrm2708

2. Feng YC, He D, Yao ZY, Klionsky DJ. The machinery of macroautophagy. Cell Res 2014; 24:24-41; PMID:24366339; http://dx.doi.org/10.1038/cr.2013.168

3. Levine B, Kroemer G. Autophagy in the pathogenesis of disease. Cell 2008; 132:27-42; PMID:18191218; http://dx.doi.org/10.1016/j.cell.2007.12.018

4. Tian Y, Li ZP, Hu WQ, Ren HY, Tian E, Zhao Y, Lu Q, Huang X, Yang P, Li X, et al. *C. elegans* screen identifies autophagy genes specific to multicellular organisms. Cell 2010; 141:1042-55; PMID:20550938; http://dx.doi.org/10.1016/j.cell.2010.04.034

5. Lu Q, Yang PG, Huang XX, Hu WQ, Guo B, Wu F, Lin L, Kovács AL, Yu L, Zhang H. The WD40 repeat PtdIns(3)P-binding protein EPG-6 regulates progression of omegasomes to autophagosomes. Dev Cell 2011; 21:343-57; PMID:21802374; http://dx.doi.org/10.1016/j.devcel.2011.06.024

6. Lu Q, Wu F, Zhang H. Aggrephagy: lessons from *C. elegans*. Biochem J 2013; 452:381-90; PMID:23725457; http://dx.doi.org/10.1042/BJ20121721

7. Zhang YX, Yan LB, Zhou Z, Yang PG, Tian E, Zhang K, Zhao Y, Li Z, Song B, Han J, et al. SEPA-1 mediates the specific recognition and degradation of P granule components by autophagy in *C. elegans*. Cell 2009; 136:308-21; PMID:19167332; http://dx.doi.org/10.1016/j.cell.2008.12.022

8. Tóth ML, Simon P, Kovács AL, Vellai T. Influence of autophagy genes on ion-channel-dependent neuronal degeneration in *Caenorhabditis elegans*. J Cell Sci 2007; 120:1134-41; http://dx.doi.org/10.1242/jcs.03401

9. Samara C, Syntichaki P, Tavernarakis N. Autophagy is required for necrotic cell death in *Caenorhabditis elegans*. Cell Death Differ 2008; 15:105-12; PMID:17901876; http://dx.doi.org/10.1038/sj.cdd.4402231

10. Meléndez A, Talloczy Z, Seaman M, Eskelinen EL, Hall DH, Levine B. Autophagy genes are essential for dauer development and life-span extension in C-elegans. Science 2003; 301:1387-91; http://dx.doi.org/10.1126/science.1087782

11. Tóth ML, Sigmond T, Borsos E, Barna J, Erdélyi P, Takacs-Vellai K, Orosz L, Kovács AL, Csikós G, Sass M, et al. Longevity pathways converge on autophagy genes to regulate He span in *Caenorhabditis elegans*. Autophagy 2008; 4:330-8; http://dx.doi.org/10.4161/auto.5618

12. Hansen M, Chandra A, Mitic LL, Onken B, Driscoll M, Kenyon C. A role for autophagy in the extension of life span by dietary restriction in C-elegans. Plos Genet 2008; 4:e24

13. Jia KL, Levine B. Autophagy is required for dietary restriction-mediated life-span extension in C-elegans. Autophagy 2007; 3:597-9; PMID:17912023; http://dx.doi.org/10.4161/auto.4989

14. Jia KL, Thomas C, Akbar M, Sun QH, Adams-Huet B, Gilpin C, Levine B. Autophagy genes protect against Salmonella typhimurium infection and mediate insulin signaling-regulated pathogen resistance. Proc Natl Acad Sci U S A 2009; 106:14564-9; PMID:19667176; http://dx.doi.org/10.1073/pnas.0813319106

15. Tian E, Wang FX, Han JH, Zhang H. epg-1 functions in the autophagy pathway and may encode a highly divergent Atg13 homolog in *C. elegans*. Autophagy 2009; 5:608-15; PMID:19377305; http://dx.doi.org/10.4161/auto.5.5.8624

16. Yang PG, Zhang H. The coiled-coil domain protein EPG-8 plays an essential role in the autophagy pathway in *C. elegans*. Autophagy 2011; 7:159-65; PMID:21116129; http://dx.doi.org/10.4161/auto.7.2.14223

17. Liang QQ, Yang PG, Tian E, Han JH, Zhang H. The *C. elegans* ATG101 homolog EPG-9 directly interacts with EPG-1/Atg13 and is essential for autophagy. Autophagy 2012; 8:1426-33; PMID:22885670; http://dx.doi.org/10.4161/auto.21163

18. Yang PG, Zhang H. You are what you eat: multifaceted functions of autophagy during *C. elegans* development. Cell Res 2014; 24:80-91; PMID:24296782; http://dx.doi.org/10.1038/cr.2013.154

19. Suzuki K, Kubota Y, Sekito T, Ohsumi Y. Hierarchy of Atg proteins in pre-autophagosomal structure organization. Genes Cells 2007; 12:209-218; PMID:17295840; http://dx.doi.org/10.1111/j.1365-2443.2007.01050.x

20. Itakura E, Mizushima N. Characterization of autophagosome formation site by a hierarchical analysis of mammalian Atg proteins. Autophagy 2010; 6:764-776; PMID:20639694; http://dx.doi.org/10.4161/auto.6.6.12709

21. Mizushima N, Yoshimori T, Levine B. Methods in mammalian autophagy research. Cell 2010; 140:313-26; PMID:20144757; http://dx.doi.org/10.1016/j.cell.2010.01.028

22. Klionsky DJ, Abdalla FC, Abeliovich H, Abraham RT, Acevedo-Arozena A, Adeli K, Agholme L, Agnello M, Agostinis P, Aguirre-Ghiso JA, et al. Guidelines for the use and interpretation of assays for monitoring autophagy. Autophagy 2012; 8:445-544; PMID:22966490

23. Kovács AL, Vellai T, Müller F. Autophagy in *Caenorhabditis elegans*. In Autophagy 2004. Klionsky DJ, editor. Eurekah.com, Landes Bioscience, Austin, Georgetown, Texas, USA 217-23.

24. Alberti A, Michelet X, Djeddi A, Legouis R. The autophagosomal protein LGG-2 acts synergistically with LGG-1 in dauer formation and longevity in *C. elegans*.

Autophagy 2010; 6:622-33; PMID:20523114; http://dx.doi.org/10.4161/auto.6.5.12252

25. Manil-Ségalen M, Lefebvre C, Jenzer C, Trichet M, Boulogne C, Satiat-Jeunemaitre B, Legouis R. The *C. elegans* LC3 acts downstream of GABARAP to degrade autophagosomes by interacting with the HOPS subunit VPS39. Dev Cell 2014; 28:43-55; http://dx.doi.org/10.1016/j.devcel.2013.11.022

26. Wu F, Li YP, Wang FX, Noda NN, Zhang H. Differential function of the two Atg4 homologues in the aggrephagy pathway in *Caenorhabditis elegans*. J Biol Chem 2012; 287:29457-67; PMID:22767594; http://dx.doi.org/10.1074/jbc.M112.365676

27. Zhang H, Wu F, Wang XW, Du HW, Wang XC, Zhang H. The two *C. elegans* ATG-16 homologs have partially redundant functions in the basal autophagy pathway. Autophagy 2013; 9: 1965-74; PMID:24185444; http://dx.doi.org/10.4161/auto.26095

28. Kang C, You YJ, Avery L. Dual roles of autophagy in the survival of *Caenorhabditis elegans* during starvation. Genes Dev 2007; 21:2161-71; PMID:17785524; http://dx.doi.org/10.1101/gad.1573107

29. Sato M, Sato K. Degradation of paternal mitochondria by fertilization-triggered autophagy in *C. elegans* Embryos. Science 2011; 334:1141-4; PMID:21998252; http://dx.doi.org/10.1126/science.1210333

30. Al Rawi S, Louvet-Vallee S, Djeddi A, Sachse M, Culetto E, Hajjar C, Boyd L, Legouis R, Galy V. Post-fertilization autophagy of sperm organelles prevents paternal mitochondrial DNA transmission. Science 2011; 334:1144-7; PMID:22033522; http://dx.doi.org/10.1126/science.1211878

31. Guo B, Liang QQ, Li L, Hu Z, Wu F, Zhang PP, Ma YF, Zhao B, Kovács AL, Zhang ZY, et al. *O*-GlcNAc-modification of SNAP-29 regulates autophagosome maturation. Nat Cell Biol 2014; 16:1215-1226..

32. Sun T, Wang X, Lu Q, Ren H, Zhang H. CUP-5, the C. elegans ortholog of the mammalian lysosomal channel protein MLN1/TRPML1, is required for proteolytic degradation in autolysosomes. Autophagy 2011; 7:1308-15; PMID:21997367; http://dx.doi.org/10.4161/auto.7.11.17759

33. Hird SN, Paulsen JE, Strome S. Segregation of germ granules in living *Caenorhabditis elegans* embryos: Cell-type-specific mechanisms for cytoplasmic localisation. Development 1996; 122:1303-12; PMID:8620857

34. Wu XY, Shi Z, Cui MX, Han M, Ruvkun G. Repression of germline RNAi pathways in somatic cells by retinoblastoma pathway chromatin complexes. Plos Genet 2012; 8:e1002542; PMID:22412383; http://dx.doi.org/10.1371/journal.pgen.1002542

35. Lin L, Yang PG, Huang XX, Zhang H, Lu Q, Zhang H. The scaffold protein EPG-7 links cargo receptor complexes with the autophagic assembly machinery. J Cell Biol 2013; 201:113-29; PMID:23530068; http://dx.doi.org/10.1083/jcb.201209098

36. Okamoto H, Thomson JN. Monoclonal-antibodies which distinguish certain classes of neuronal and supporting cells in the nervous-tissue of the nematode Caenorhabditis-elegans. J Neurosci 1985; 5:643-53; PMID:3882896

37. Ward S, Roberts TM, Strome S, Pavalko FM, Hogan E. Monoclonal-antibodies that recognize a polypeptide antigenic determinant shared by multiple Caenorhabditis elegans sperm-specific proteins. J Cell Biol 1986; 102:1778-86; PMID:2422180; http://dx.doi.org/10.1083/jcb.102.5.1778

38. Tsang WY, Lemire BD. Stable heteroplasmy but differential inheritance of a large mitochondrial DNA deletion in nematodes. Biochem Cell Biol 2002; 80:645-54; PMID:12440704; http://dx.doi.org/10.1139/o02-135

39. Guo B, Huang J, Wu WX, Feng D, Wang XC, Chen YY, Zhang H. The nascent polypeptide-associated complex is essential for autophagic flux. Autophagy 2014; 10, 1738-1748; PMID:25126725; http://dx.doi.org/10.4161/auto.29638

40. Guo B, Huang XX, Zhang PP, Qi LX, Liang QQ, Zhang XB, Huang J, Fang B, Hou W, Han J, et al. Genome-wide screen identifies signaling pathways that regulate autophagy during *Caenorhabditis elegans* development. Embo Rep 2014; 15:705-13; PMID:24764321

41. Oka T, Futai M. Requirement of V-ATPase for ovulation and embryogenesis in Caenorhabditis elegans. J Biol Chem. 2000; 275:29556-61; PMID:10846178; http://dx.doi.org/10.1074/jbc.M002756200

42. Pivtoraiko VN, Harrington AJ, Mader BJ, Luker AM, Caldwell GA, Caldwell KA, Roth KA, Shacka JJ. Low-dose bafilomycin attenuates neuronal cell death associated with autophagy-lysosome pathway dysfunction. J Neurochem. 2010; 114:1193-204; PMID:20534000

43. Lapierre LR, De Magalhaes Filho CD, McQuary PR, Chu CC, Gelino S, Ong B, Davis AE, Irazoqui JE, et al. The TFEB orthologue HLH-30 regulates autophagy and modulates longevity in Caenorhabditis elegans. Nat Commun. 2013; 4:2267; PMID:23925298

44. Heestand BN, Shen Y, Liu W, Magner DB, Storm N, Meharg C, Habermann B, Antebi A. Dietary restriction induced longevity is mediated by nuclear receptor NHR-62 in Caenorhabditis elegans. PLoS Genet. 2013; 9:e1003651; PMID:23935515; http://dx.doi.org/10.1371/journal.pgen.1003651

45. Settembre C, DeCegli R, Mansueto G, Saha PK, Vetrini F, Visvikis O, Huynh T, Carissimo A, Palmer D, Klisch TJ, et al. TFEB controls cellular lipid metabolism through a starvation-induced autoregulatory loop. Nat Cell Biol. 2013; 15:647-58; PMID:23604321; http://dx.doi.org/10.1038/ncb2718

46. O'Rourke EJ, Ruvkun G. MXL-3 and HLH-30 transcriptionally link lipolysis and autophagy to nutrient availability. Nat Cell Biol 2013; 15:668-76; PMID:23604316; http://dx.doi.org/10.1038/ncb2741

47. Sigmond T, Feher J, Baksa A, Pasti G, Palfia Z, Takacs-Vellai K, Kovács J, Vellai T, Kovács AL. Qualitative and quantitative characterization of autophagy in *Caenorhabditis Elegans* by electron microscopy. Autophagy: Lower Eukaryotes and Non-Mammalian Systems, Pt A 2008; 451:467-91.

48. Kovács AL, László L, Kovács J. Effect of amino-acids and cycloheximide on changes caused by vinblastine, leupeptin and methylamine in the autophagic lysosomal system of mouse hepatocytes in vivo. Exp Cell Res 1985; 157:83-94; http://dx.doi.org/10.1016/0014-4827(85)90154-5

49. Kovács J, László L, Kovács AL. Regression of autophagic vacuoles in pancreatic acinar, seminal-vesicle epithelial, and liver parenchymal cells: a comparative morphometric study of the effect of vinblastine and leupeptin followed by cycloheximide treatment. Exp Cell Res 1988; 174:244-51; http://dx.doi.org/10.1016/0014-4827(88)90158-9

50. You YJ, Kim J, Cobb M, Avery L. Starvation activates MAP kinase through the muscarinic acetylcholine pathway in *Caenorhabditis elegans* pharynx. Cell Metabolism 2006; 3:237-45; PMID:16581001; http://dx.doi.org/10.1016/j.cmet.2006.02.012

51. Cassada RC, Russell RL. The dauerlarva, a post-embryonic developmental variant of the nematode Caenorhabditis elegans. Dev Biol. 1975; 46:326-42; PMID:1183723

52. Vowels JJ, Thomas JH. Genetic analysis of chemosensory control of dauer formation in Caenorhabditis elegans. Genetics 1992; 130:105-23; PMID:1732156

53. Klass M, Hirsh D. Non-ageing developmental variant of Caenorhabditis elegans. Nature 1976; 260:523-5; PMID:1264206; http://dx.doi.org/10.1038/260523a0

54. Hu PJ. Dauer. Worm Book 2007 Aug; 8:1-19.

55. Kenyon C. The genetics of ageing. Nature 2010; 464:504-12; PMID:20336132; http://dx.doi.org/10.1038/nature08980

56. Kovács AL, Zhang H. Role of autophagy in *Caenorhabditis elegans*. Febs Letters 2010; 584:1335-41; http://dx.doi.org/10.1016/j.febslet.2010.02.002

57. Gelino S, Hansen M. Autophagy - an emerging anti-aging mechanism. J Clin Exp Pathol. 2012; Suppl 4. pii: 006.

58. Hars ES, Qi H, Ryazanov AG, Jin S, Cai L, Hu C, Liu LF. Autophagy regulates ageing in C. elegans. Autophagy 2007; 3:93-5; PMID:17204841; http://dx.doi.org/10.4161/auto.3636

59. Lapierre LR, Gelino S, Melendez A, Hansen M. Autophagy and lipid metabolism coordinately modulate life span in germline-less *C. elegans*. Current Biology 2011; 21:1507-14; PMID:21906946; http://dx.doi.org/10.1016/j.cub.2011.07.042

60. Derrien B, Baumberger N, Schepetilnikov M, Viotti C, De Cillia J, Ziegler-Graff V, Isono E, Schumacher K, Genschik P. Degradation of the antiviral component ARGONAUTE1 by the autophagy pathway. Proc Natl Acad Sci U S A 2012; 109:15942-6; PMID:23019378; http://dx.doi.org/10.1073/pnas.1209487109

61. Gibbings D, Mostowy S, Jay F, Schwab Y, Cossart P, Voinnet O. Selective autophagy degrades DICER and AGO2 and regulates miRNA activity. Nat Cell Biol 2012; 14:1314-21; PMID:23143396; http://dx.doi.org/10.1038/ncb2611

62. Zhang PP, Zhang H. Autophagy modulates miRNA-mediated gene silencing and selectively degrades AIN-1/GW182 in C-elegans. Embo Rep 2013; 14:568-76; PMID:23619095; http://dx.doi.org/10.1038/embor.2013.53

63. Johnston RJ, Hobert O. A microRNA controlling left/right neuronal asymmetry in *Caenorhabditis elegans*. Nature 2003; 426:845-9; PMID:14685240; http://dx.doi.org/10.1038/nature02255

64. Sarin S, O'Meara MM, Flowers EB, Antonio C, Poole RJ, Didiano D, Johnston RJ Jr, Chang S, Narula S, Hobert O. Genetic screens for *Caenorhabditis elegans* mutants defective in left/right asymmetric neuronal fate specification. Genetics 2007; 176:2109-30; PMID:17717195; http://dx.doi.org/10.1534/genetics.107.075648

65. Sulston JE, Horvitz HR. Post-embryonic cell lineages of the nematode, *Caenorhabditis elegans*. Dev Biol 1977; 56:110-56; PMID:838319; http://dx.doi.org/10.1016/0012-1606(77)90158-0

66. Huang S, Jia K, Wang Y, Zhou Z, Levine B. Autophagy genes function in apoptotic cell corpse clearance during *C. elegans* embryonic development. Autophagy 2013; 9:138-49; PMID:23108454; http://dx.doi.org/10.4161/auto.22352

67. Cheng SY, Wu YW, Lu Q, Yan JC, Zhang H, Wang XC. Autophagy genes coordinate with the class II PI/PtdIns 3-kinase PIKI-1 to regulate apoptotic cell clearance in *C. elegans*. Autophagy 2013; 9:2022-32; PMID:24165672; http://dx.doi.org/10.4161/auto.26323

68. Gumienny TL, Lambie E, Hartwieg E, Horvitz HR, Hengartner MO. Genetic control of programmed cell death in the *Caenorhabditis elegans* hermaphrodite germline. Development 1999; 126:1011-22; PMID:9927601

69. Gartner A, Milstein S, Ahmed S, Hodgkin J, Hengartner MO. A conserved checkpoint pathway mediates DNA damage-induced apoptosis and cell cycle arrest in *C. elegans*. Molecular Cell 2000; 5:435-43; PMID:10882129; http://dx.doi.org/10.1016/S1097-2765(00)80438-4

70. Gartner A, Boag PR, Blackwell TK. Germline survival and apoptosis. Worm Book. 2008 Sep 4:1-20.

71. Wang HB, Lu Q, Cheng SY, Wang XC, Zhang H. Autophagy activity contributes to programmed cell death in *Caenorhabditis elegans*. Autophagy 2013; 9:1975-82; PMID:24185352; http://dx.doi.org/10.4161/auto.26152

72. Singh R, Kaushik S, Wang YJ, Xiang YQ, Novak I, Komatsu M, Tanaka K, Cuervo AM, Czaja MJ. Autophagy regulates lipid metabolism. Nature 2009; 458:1131-5; PMID:19339967; http://dx.doi.org/10.1038/nature07976

73. Wählby C, Lee-Conery A, Bray MA, Kamentsky L, Larkins-Ford J, Sokolnicki K, Veneskey M, Michaels

K, Carpenter AE, O'Rourke EJ. High and low through-put quantitative analysis of lipid metabolism in *C. elegans*. Methods 2014; 68:492-9; http://dx.doi.org/10.1016/j.ymeth.2014.04.017

74. Aballay A, Ausubel FM. *Caenorhabditis elegans* as a host for the study of host-pathogen interactions. Curr Opin Microbiol 2002; 5:97-101; PMID:11834377; http://dx.doi.org/10.1016/S1369-5274(02)00293-X

75. Kurz CL, Ewbank JJ. *Caenorhabditis elegans*: An emerging genetic model for the study of innate immunity. Nat Rev Genet 2003; 4:380-90; PMID:12728280; http://dx.doi.org/10.1038/nrg1067

76. Millet ACM, Ewbank JJ. Immunity in *Caenorhabditis elegans*. Curr Opin Immunol 2004; 16:4-9; PMID:14734103; http://dx.doi.org/10.1016/j.coi.2003.11.005

77. Mylonakis E, Aballay A. Worms and flies as genetically tractable animal models to study host-pathogen interactions. Infect Immun 2005; 73:3833-41; PMID:15972468; http://dx.doi.org/10.1128/IAI.73.7.3833-3841.2005

78. Aballay A, Drenkard E, Hilbun LR, Ausubel FM. *Caenorhabditis elegans* innate immune response triggered by Salmonella enterica requires intact LPS and is mediated by a MAPK signaling pathway. Curr Biol 2003; 13:47-52; PMID:12526744; http://dx.doi.org/10.1016/S0960-9822(02)01396-9

79. Aballay A, Yorgey P, Ausubel FM. Salmonella typhimurium proliferates and establishes a persistent infection in the intestine of *Caenorhabditis elegans*. Curr Biol 2000; 10:1539-42; PMID:11114525; http://dx.doi.org/10.1016/S0960-9822(00)00830-7

80. Labrousse A, Chauvet S, Couillault C, Kurz CL, Ewbank JJ. *Caenorhabditis elegans* is a model host for Salmonella typhimurium. Curr Biol 2000; 10:1543-5; PMID:11114526; http://dx.doi.org/10.1016/S0960-9822(00)00833-2

81. Benjamin JL, Sumpter R, Levine B, Hooper LV. Intestinal epithelial autophagy is essential for host defense against invasive bacteria. Cell Host Microbe 2013; 13:723-34; PMID:23768496; http://dx.doi.org/10.1016/j.chom.2013.05.004

82. Birmingham CL, Smith AC, Bakowski MA, Yoshimori T, Brumell JH. Autophagy controls Salmonella infection in response to damage to the Salmonella-containing vacuole. J Biol Chem 2006; 281:11374-83; PMID:16495224; http://dx.doi.org/10.1074/jbc.M509157200

83. Conway KL, Kuballa P, Song JH, Patel KK, Castoreno AB, Yilmaz OH, Jijon HB, Zhang M, Aldrich LN, Villablanca EJ, et al. Atg16l1 is required for autophagy in intestinal epithelial cells and protection of mice from salmonella infection. Gastroenterology 2013; 145:1347-57; PMID:23973919; http://dx.doi.org/10.1053/j.gastro.2013.08.035

84. Curt A, Zhang JL, Minnerly J, Jia KL. Intestinal autophagy activity is essential for host defense against Salmonella typhimurium infection in *Caenorhabditis elegans*. Dev Comp Immunol 2014; 45:214-8; PMID:24674884; http://dx.doi.org/10.1016/j.dci.2014.03.009

85. Ogura K, Wicky C, Magnenat L, Tobler H, Mori I, Müller F, Ohshima Y. *Caenorhabditis elegans* unc-51 gene required for axonal elongation encodes a novel serine/threonine kinase. Genes Dev. 1994; 8:2389-400; PMID:7958904; http://dx.doi.org/10.1101/gad.8.20.2389

86. Ruck A, Attonito J, Garces KT, Núnez L, Palmisano NJ, Rubel Z, Bai Z, Nguyen KC, Sun L, Grant BD, et al. The Atg6/Vps30/Beclin 1 ortholog BEC-1 mediates endocytic retrograde transport in addition to autophagy in C. elegans. Autophagy 2011; 7:386-400; PMID:21183797; http://dx.doi.org/10.4161/auto.7.4.14391

87. Roggo L, Bernard V, Kovacs AL, Rose AM, Savoy F, Zetka M, Wymann MP, Müller F. Membrane transport in Caenorhabditis elegans: an essential role for VPS34 at the nuclear membrane. EMBO J. 2002; 21:1673-83; http://dx.doi.org/10.1093/emboj/21.7.1673

88. Cheeks RJ, Canman JC, Gabriel WN, Meyer N, Strome S, Goldstein B. *C. elegans* PAR proteins function by mobilizing and stabilizing asymmetrically localized protein complexes. Curr Biol. 2004; 14:851-62; PMID:15186741; http://dx.doi.org/10.1016/j.cub.2004.05.022

89. Kawasaki I, Shim YH, Kirchner J, Kaminker J, Wood WB, Strome S. PGL-1, a predicted RNA-binding component of germ granules, is essential for fertility in C. elegans. Cell 1998; 94:635-45; PMID:9741628; http://dx.doi.org/10.1016/S0092-8674(00)81605-0

90. Kawasaki I, Amiri A, Fan Y, Meyer N, Dunkelbarger S, Motohashi T, Karashima T, Bossinger O, Strome S. The PGL family proteins associate with germ granules and function redundantly in Caenorhabditis elegans germline development. Genetics 2004; 167:645-61; PMID:15238518; http://dx.doi.org/10.1534/genetics.103.023093

91. Wilkinson DS, Jariwala JSAnderson E, Mitra K, Meisenhelder J, Chang JT, Ideker T, Hunter T, Nizet V, Dillin A et al. Phosphorylation of LC3 by the Hippo Kinases STK3/STK4 is essential for autophagy. Mol Cell 2015; 57:55-68; doi: 10.1016/j.molcel.2014.11.019